A MULTIVARIATE SPLINE BASED COLLOCATION METHOD FOR NUMERICAL SOLUTION OF PARTIAL DIFFERENTIAL EQUATIONS*

MING-JUN LAI† AND JINSIL LEE‡

Abstract. We propose a collocation method based on multivariate polynomial splines over triangulation or tetrahedralization for numerical solution of partial differential equations. We start with a detailed explanation of the method for the Poisson equation and then extend the study to the second order elliptic PDE in non-divergence form. We shall show that the numerical solution can approximate the exact PDE solution very well. Then we present a large amount of numerical experimental results to demonstrate the performance of the method over the 2D and 3D settings. In addition, we present a comparison with the existing multivariate spline methods in [1] and [12] to show that the new method produces a similar and sometimes more accurate approximation in a more efficient fashion.

Key words. Collocation Method, Multivariate Splines, the Poisson equation, the second order elliptic PDE, Non-divergence form

AMS subject classifications. 65N30, 65N12, 35J15, 35D35

1. Introduction. In this paper, we propose and study a new collocation method based on multivariate splines for numerical solution of partial differential equations over polygonal domain in $\mathbb{R}^d$ for $d \geq 2$. Instead of using a second order elliptic equation in divergence form:

$$\left\{ \begin{array}{ll} -\sum_{i,j=1}^d \frac{\partial}{\partial x_i}(a^{ij}(x)\frac{\partial}{\partial x_j}u) + \sum_{i=1}^d b^i(x)\frac{\partial}{\partial x_i}u + c^1(x)u &= f, \quad x \in \Omega \subset \mathbb{R}^d, \\ u &= g, \quad \text{on } \partial\Omega \end{array} \right. \tag{1.1}$$

which is often used for various finite element methods, we discuss in this paper a more general form of second order elliptic PDE in non-divergence form:

$$\left\{ \begin{array}{ll} \sum_{i,j=1}^d a^{ij}(x)\frac{\partial}{\partial x_i}\frac{\partial}{\partial x_j}u + \sum_{i=1}^d b^i(x)\frac{\partial}{\partial x_i}u + c(x)u &= f, \quad x \in \Omega \subset \mathbb{R}^d, \\ u &= g, \quad \text{on } \partial\Omega, \end{array} \right. \tag{1.2}$$

where the PDE coefficient functions $a^{ij}(x), i,j = 1, \cdots, d$ are in $L^\infty(\Omega)$ and satisfy the standard elliptic condition. In addition, when $d \geq 2$, we shall assume the so-called Cordés condition, see (4.3) in a later section or see [18]. Numerical solutions to the 2nd order PDE in the non-divergence form have been studied extensively recently. See some studies in [18], [12], [15], [19], [17], and etc.. The method in this paper provides a new and more effective approach.

In this paper, we shall mainly use the Sobolev space $H^2(\Omega)$ which is dense in $H^1(\Omega)$. It is known when Ω is convex (cf. [6]), the solution to the Poisson equation will be $H^2(\Omega)$. Recently, the researchers in [5] showed that when Ω has an uniformly positive reach, the solution of (1.2) with zero boundary condition will be in $H^2(\Omega)$. Domains of uniformly positive reach, e.g. star-shaped domain and domains with holes are shown in [5]. Many more domains than convex domains can have H^2 solution.

*Submitted to the editors DATE.

†Department of Mathematics, University of Georgia, Athens, GA 30602 (mjlai@uga.edu, http://alpha.math.uga.edu/~mjlai/).

‡Department of Mathematics, University of Georgia, Athens, GA 30602 (Jinsil.Lee@uga.edu)

This manuscript is for review purposes only.

This enables us to consider the idea of collocation method. For any $u \in H^2(\Omega)$, we use the standard norm

$$\|u\|_{H^2} = \|u\|_{L^2(\Omega)} + \|\nabla u\|_{L^2(\Omega)} + \sum_{i,j=1}^{d} \|\frac{\partial}{\partial x_i}\frac{\partial}{\partial x_j} u\|_{L^2(\Omega)} \tag{1.3}$$

for all u on $H^2(\Omega)$ and the semi-norm

$$|u|_{H^2} = \sum_{i,j=1}^{d} \|\frac{\partial}{\partial x_i}\frac{\partial}{\partial x_j} u\|_{L^2(\Omega)}. \tag{1.4}$$

Since we will use multivariate spline functions to approximate the solution $u \in H^2(\Omega)$, we use C^r smooth spline functions with $r \geq 1$ and the degree D of splines sufficiently large satisfying $D \geq 3r+2$ in $\mathbb{R}^2$ and $D \geq 6r+3$ in $\mathbb{R}^3$. Indeed, how to use such spline functions has been explained in [1], [16], and [17], and etc..

Certainly, the PDE in (1.2) includes the standard Poisson equation as a special case.

$$\begin{cases} -\Delta u &= f, \quad x \in \Omega \subset \mathbb{R}^d, \\ u &= g, \quad \text{on } \partial\Omega. \end{cases} \tag{1.5}$$

For convenience, we shall begin with this equation to explain our collocation method and establish the method by showing that the numerical solution is convergent to the true solution. As mentioned above, we shall use C^r spline functions with $r \geq 1$ to do so. In addition, we shall use the so-called domain points (cf. [10]) to be the collocation points (they will be explained in the next section). For simplicity, let us say s is a C^2 spline of degree D defined on a triangulation $\triangle$ of Ω and $\xi_i, i = 1, \cdots, N$ are the domain points of $\triangle$ and degree $D' > 0$, where D' may be different from D. Our multivariate spline based collocation method is to seek a spline function s satisfying

$$\begin{cases} -\Delta s(\xi_i) &= f(\xi_i), \quad \xi_i \in \Omega \subset \mathbb{R}^d, \\ s(\xi_i) &= g(\xi_i), \quad \xi_i \in \partial\Omega. \end{cases} \tag{1.6}$$

As a multivariate spline space (to be defined in the next section) is a linear vector space which is spanned by a set of basis functions. Since it is difficult to construct locally supported basis functions in $C^r(\Omega)$ with $r \geq 1$, we will begin with discontinuous spline space $s \in S_D^{-1}(\triangle)$ and then add the smoothness conditions which are written as $H\mathbf{s} = 0$, where $\mathbf{s}$ is the coefficient vector of s and H is the matrix consisting of all smoothness condition across each interior edge of a triangulation/tetrahedralization. We mainly look for the coefficient vector $\mathbf{s}$ such that the spline s with coefficient vector $\mathbf{s}$ satisfies (1.6). Clearly, (1.6) leads to a linear system which may not have a unique solution. It may be an over-determined linear system if $D' \geq D$ or an under-determined linear system if $D' < D$. Our method is to use a least squares solution if the system is overdetermined or a sparse solution if the system is under-determined (cf. [13]).

To establish the convergence of the collocation solution s as the size of $\triangle$ goes to zero, we define a new norm $\|u\|_L$ on $H^2(\Omega)$ for the Poisson equation as follows.

$$\|u\|_L = \|\Delta u\|_{L^2(\Omega)} + \|u\|_{L^2(\partial\Omega)}. \tag{1.7}$$

We mainly show that the new norm is equivalent on the standard norm on $H^2(\Omega)$. That is, THEOREM 1.1. *Suppose $\Omega \subset \mathbb{R}^d$ be a bounded domain. Suppose the closure of Ω is a multiple-strictly-star-shaped domain (see Definition 2.4). Then there exist two positive constants A and B such that*

$$A\|u\|_{H^2} \leq \|u\|_L \leq B\|u\|_{H^2}, \quad \forall u \in H^2(\Omega). \tag{1.8}$$

See the proof of Theorem 3.3 in a later section. Letting $u \in H^2(\Omega)$ be the solution of (1.5) and u_s be the spline solution of (1.6), we use the first inequality above to have

$$A\|u - u_s\|_{H^2} \leq \|u - u_s\|_L.$$

It can be seen from (1.6) that $\|u - u_s\|_L^2 = \int_\Omega (\Delta(u - u_s))^2 dx + \int_{\partial\Omega} |u_s - u|^2 = \int_\Omega (f + \Delta u_s)^2 dx + \int_{\partial\Omega} |u_s - g|^2$ will be small for a sufficiently large amount of collocation points and distributed evenly, our Theorem 1.1 implies that $\|u - u_s\|_{H^2}$ is small. Furthermore, we will show

$$\|u - u_s\|_{L^2(\Omega)} \leq C|\triangle|^2\|u - u_s\|_L \text{ and } \|\nabla(u - u_s)\|_{L^2(\Omega)} \leq C|\triangle|\|u - u_s\|_L \tag{1.9}$$

for a positive constant C, where $|\triangle|$ is the size of triangulation or tetrahedralization $\triangle$ under the assumption that $u - u_s = 0$ on $\partial\Omega$. These will establish the multivariate spline based collocation method for the Poisson equation.

In general, we let $\mathcal{L}$ be the PDE operator in (1.10). Note that we begin with the second order term of the PDE just for convenience.

$$\begin{cases} \sum_{i,j=1}^d a^{ij}(x) \frac{\partial}{\partial x_i} \frac{\partial}{\partial x_j} u & = f, \quad x \in \Omega \subset \mathbb{R}^d, \\ u & = g, \quad \text{on } \partial\Omega, \end{cases} \tag{1.10}$$

We shall similarly define a new norm associated with the PDE (1.10):

$$\|u\|_{\mathcal{L}} = \|\mathcal{L}(u)\|_{L^2(\Omega)} + \|u\|_{L^2(\partial\Omega)}. \tag{1.11}$$

Similarly we will show the following.

THEOREM 1.2. *Suppose $\Omega \subset \mathbb{R}^d$ be a bounded domain. Suppose the closure of Ω is of uniformly positive reach $r_\Omega > 0$ and a multiple strictly star-shaped domain. Suppose that the second order partial differential equation in (1.10) is elliptic, i.e. satisfying (4.2) and satisfies the Cordés condition if $d \geq 2$. There exist two positive constants A_1 and B_1 such that*

$$A_1\|u\|_{H^2} \leq \|u\|_{\mathcal{L}} \leq B_1\|u\|_{H^2}, \quad \forall u \in H^2(\Omega). \tag{1.12}$$

See a proof in a section later. Similar to the Poisson equation setting, this result will enable us to establish the convergence of the spline based collocation method for the second order elliptic PDE in non-divergence form. Also, we will have the improved convergence similar to (1.9).

There are a few advantages of the collocation methods over the traditional finite element methods, discontinuous Galerkin methods, virtual element methods, and etc.. For example, no numerical quadrature is needed for the computation. For another example, it is more flexible to deal with the discontinuity arising from the PDE coefficients as one may easily adjust the locations of some collocation points close to the discontinuity. A clear advantage of multivariate splines is that one can increase the accuracy of the approximation by increasing the degree of splines and/or the number of collocation points which can be cheaper than finding the solution over a uniform refinement of the underlying triangulation or tetrahedralization within the memory budget of a computer.

We shall provide many numerical results in 2D and 3D to demonstrate how well the spline based collocation methods can perform. Mainly, we would like to show the performance of solutions under the various settings: (1) the PDE coefficients are smooth or not very smooth, (2) the PDE solutions are smooth or not very smooth, (3) the domain of interest is star-shaped or non-star-shaped, even very complicated domain such such the human head used in the numerical experiment in this paper, and (4) the dimension d can be 2 or 3. In particular, using splines of high degree enables us to find a numerical solution with high accuracy. We are not able to show the rate of convergence in terms of the size of triangulation. Instead, we present the accuracy of spline solutions for various kinds of testing functions. In addition, we shall compare with the existing methods in [1] and [12] to demonstrate that the multivariate spline based collocation method can be better in the sense that it is more accurate and more efficient under the assumption that the associated collocation matrices are generated beforehand. Finally, we remark that we have extended our study to the biharmonic equation, i.e. Stokes equations and Navier-Stokes equations as well as the Monge-Ampére equation. These will leave to a near future publication, e.g. [14].

2. Preliminary on Multivariate Splines and the Trace Inequality. In this section, we first quickly summarize the essentials of multivariate splines and then present an elementary discussion on the trace inequality which will be used in later sections.

2.1. Multivariate Splines. We begin with bivariate spline functions. For any polygonal domain $\Omega \subset \mathbb{R}^d$ with $d = 2$, let $\triangle := \{T_1, \cdots, T_n\}$ be a triangulation of Ω which is a collection of triangles and $\mathcal{V}$ be the set of vertices of $\triangle$. For a triangle $T = (v_1, v_2, v_3) \in \Omega$, we define the barycentric coordinates (b_1, b_2, b_3) of a point $(x, y) \in \Omega$. These coordinates are the solution to the following system of equations

$$\begin{aligned} b_1 + b_2 + b_3 &= 1 \\ b_1 v_{1,x} + b_2 v_{2,x} + b_3 v_{3,x} &= x \\ b_1 v_{1,y} + b_2 v_{2,y} + b_3 v_{3,y} &= y \end{aligned}$$

and are nonnegative if $(x, y) \in T$. We use the barycentric coordinates to define the Bernstein polynomials of degree D:

$$B^T_{i,j,k}(x, y) := \frac{k!}{i!j!k!} b_1^i b_2^j b_3^k, \ i + j + k = D,$$

which form a basis for the space $\mathcal{P}_D$ of polynomials of degree D. Therefore, we can represent all $s \in \mathcal{P}_D$ in B-form:

$$s|_T = \sum_{i+j+k=D} c_{ijk} B^T_{ijk}, \forall T \in \triangle,$$

where the B-coefficients $c_{i,j,k}$ are uniquely determined by s. Moreover, for given $T = (v_1, v_2, v_3) \in \triangle$,we define the associated set of domain points to be

$$\mathcal{D}_{D',T} := \{\frac{iv_1 + jv_2 + kv_3}{D'}\}_{i+j+k=D'}. \tag{2.1}$$

We define the spline space $S^{-1}_D(\triangle) := \{s|_T \in \mathcal{P}_D, T \in \triangle\}$, where T is a triangle in a triangulation $\triangle$ of Ω. We use this piecewise polynomial space to define the space

$\mathcal{S}^r_D := C^r(\Omega) \cap S^{-1}_D(\triangle)$. This can be achieved through the smoothness conditions on the coefficients of $s \in S^{-1}_D(\triangle)$. Let $\mathbf{s}$ be the coefficient vector of s and H be the matrix which consists of the smoothness conditions across each interior edge of $\triangle$. It is known that $H\mathbf{s} = 0$ if and only if $s \in C^r(\Omega)$ (cf. [10]).

Computations involving splines written in B-form can be performed easily according to [1] and [16]. In fact, these spline functions have numerically stable, closed-form formulas for differentiation, integration, and inner products. If $D \geq 3r+2$, spline functions on quasi-uniform triangulations have optimal approximation power.

LEMMA 2.1. *([Lai and Schumaker, 2007[10]]) Let $k \geq 3r+2$ with $r \geq 1$. Suppose $\triangle$ is a quasi-uniform triangulation of Ω. Then for every $u \in W^{k+1}_q(\Omega)$, there exists a quasi-interpolatory spline $s_u \in \mathcal{S}^r_k(\triangle)$ such that*

$$||D^\alpha_x D^\beta_y (u - s_u)||_{q,\Omega} \leq C|\triangle|^{k+1-\alpha-\beta}|u|_{k+1,q,\Omega}$$

for a positive constant C dependent on u, r, k and the smallest angle of $\triangle$, and for all $0 \leq \alpha + \beta \leq k$ with

$$|u|_{k,q,\Omega} := (\sum_{a+b=k} ||D^a_x D^b_y u||^q_{L^q(\Omega)})^{\frac{1}{q}}.$$

Similarly, for trivariate splines, let $\Omega \subset \mathbb{R}^3$ and $\triangle$ be a tetrahedralization of Ω. We define a trivariate spline just like bivariate splines by using Bernstein-Bźier polynomials defined on each tetrahedron $t \in \triangle$. Letting

$$\mathcal{S}^r_D(\triangle) = \{s \in C^r(\Omega) : s|_t \in \mathbb{P}_D, t \in \triangle\} = C^r(\Omega) \cap S^{-1}_D(\triangle)$$

be the spline space of degree D and smoothness $r \geq 0$, each $s \in \mathcal{S}^r_D(\triangle)$ can be rewritten as

$$s(x)|_t = \sum_{i+j+k+\ell=D} c^t_{ijk\ell} B^t_{ijk\ell}(x), \quad \forall t \in \triangle,$$

where $B^t_{ijk\ell}$ are Bernstein-Bźier polynomials (cf. [1], [10], [16]) which are nonzero on t and zero otherwise. Approximation properties of trivariate splines can be found in [11] and [8].

How to use them to solve partial differential equations based on the weak formulation like the finite element method has been discussed in [1] and [16]. We leave the detail to these references.

2.2. The Trace Inequality. We first recall the trace theorem from [4] that

THEOREM 2.2. *Suppose that Ω is a bounded domain with $C^{1,1}$ boundary. For $u \in H^1(\Omega)$*

$$\|u\|_{L^2(\partial\Omega)} \leq C(\|u\|_{L^2(\Omega)} + \|\nabla u\|_{L^2(\Omega)}) \tag{2.2}$$

for a positive constant C independent of u.

As the domain Ω of interest may not have a $C^{1,1}$ boundary, we would like to have this inequality for polygonal domains. Let us begin with the following trivial identity:

$$\mathrm{div}(\alpha|u|^2) = \mathrm{div}(\alpha)(u^2) + 2\alpha \cdot u\nabla u \tag{2.3}$$

for any vector function $\alpha \in C^1(\Omega)^d$. Integrating the above identity over Ω, we use the divergence theorem to have

LEMMA 2.3. *For any $u \in H^1(\Omega)$ and any vector $\alpha \in C(\Omega)^d$, one has*

$$\int_\Omega (div\,\alpha)|u|^2 + 2\int_\Omega u(\alpha\cdot\nabla u) = \int_{\partial\Omega} \alpha\cdot\mathbf{n}|u|^2. \tag{2.4}$$

We begin with the concept of strictly star-shaped domains introduced in [3]. In fact, we relax the condition of strictly star-shaped domain a little bit to make it more useful for application.

DEFINITION 2.4. *A bounded domain $\Omega \subset \mathbb{R}^d$ is a strictly star-shaped domain if it has a piecewise linear or smooth boundary and there exist a point $\mathbf{x}_0 \in \Omega$ and a positive constant $\gamma_\Omega > 0$ depending only on Ω such that*

$$(\mathbf{x}-\mathbf{x}_0)\cdot\mathbf{n} \ge \gamma_\Omega > 0, \quad \forall \mathbf{x} \in \partial\Omega, a.e., \tag{2.5}$$

where $\mathbf{n}$ stands for the normal direction of the boundary $\partial\Omega$ and a.e. stands for almost everywhere. When $\gamma_\Omega = 0$, Ω is a star-shaped domain. Furthermore, we say a domain Ω multiple-strictly-star-shaped domain if Ω is able to be decomposed into the union of a finitely many strictly star-shaped sub-domains, i.e. $\overline{\Omega} = \bigcup_{i=1}^{\ell} \overline{\Omega_i}$ with Ω_i being a strictly star-shaped domain for $i = 1, \cdots, \ell$ and $\Omega_i \cap \Omega_j = \emptyset$ for $i \neq j, i, j = 1, \cdots, \ell$.

When Ω is a strictly star-shaped domain with center $\mathbf{x}_0$ and $\gamma_\Omega > 0$, we use $\alpha = \mathbf{x}-\mathbf{x}_0$ in the result of Lemma 2.3 to have

$$d\int_\Omega |u|^2 + 2\int_\Omega u((\mathbf{x}-\mathbf{x}_0)\cdot\nabla u) = \int_{\partial\Omega}(\mathbf{x}-\mathbf{x}_0)\cdot\mathbf{n}|u|^2 \ge \gamma_\Omega\int_{\partial\Omega}|u|^2. \tag{2.6}$$

Now we apply Cauchy-Schwarz inequality to the second term on the left-hand side above to have

$$\gamma_\Omega\int_{\partial\Omega}|u|^2 \le d\int_\Omega |u|^2 + |\Omega|\sqrt{\int_\Omega |u|^2}\sqrt{\int_\Omega |\nabla u|^2} \le C_1\int_\Omega |u|^2 + C_2\int_\Omega |\nabla u|^2 \tag{2.7}$$

and hence, taking a square root both sides, we have a proof of (2.2) for a strictly star-shaped domain Ω.

When Ω is a multiple-strictly star-shaped domain, we simply apply Lemma 2.3 to each Ω_i. Letting $\gamma_\Omega = \min\{\gamma_{\Omega_i}, i = 1, \cdots, \ell\}$ and $\partial\Omega$ is a subset of $\bigcup_i \partial\Omega_i$, we use the

$$\begin{aligned} \gamma_\Omega\int_{\partial\Omega}|u|^2 &\le \sum_{i=1}^{\ell}\gamma_{\Omega_i}\int_{\partial\Omega_i}|u|^2 \le \sum_{i=1}^{\ell} C_1\int_{\Omega_i}|u|^2 + C_2\int_{\Omega_i}|\nabla u|^2 \\ &= C_1\int_\Omega |u|^2 + C_2\int_\Omega |\nabla u|^2. \end{aligned} \tag{2.8}$$

Taking a square root both sides of the inequality yields (2.2). Clearly, we can decompose a polygonal domain Ω into a triangulation/tetrahedralization. As each triangle and each tetrahedron is a strictly star-shaped domain, we use the above discussion to conclude

THEOREM 2.5. *Suppose that Ω is a polygonal domain. For any $u \in H^1(\Omega)$ one has the trace inequality (2.2).*

The same holds for a domain Ω with a curvy triangulation $\triangle$, i.e. a triangulation with curve boundary.

3. A Splined Based Collocation Method for the Poisson Equation. Let us explain a collocation method based on bivariate splines/trivariate splines for a solution of the Poisson equation (1.5). For convenience, we simply explain our method when $d = 2$ in this section. Numerical results in the settings of $d = 2$ and $d = 3$ will be given in a later section.

For given $\triangle$ be a triangulation, we choose a set of domain points $\{\xi_i\}_{i=1,\cdots,N}$ explained in the previous section as collocation points and find the coefficient vector $\mathbf{c}$ of spline function $s = \sum_{t\in\triangle} \sum_{i+j+k=D} c^t_{ijk} B^t_{ijk}$ satisfying the following equation at those points

$$\begin{cases} -\sum_{t\in\triangle}\sum_{i+j+k=D} c^t_{ijk}\Delta B^t_{ijk}(\xi_i) & = f(\xi_i), \quad \xi_i \in \Omega \subset \mathbb{R}^2 \\ s(\xi_i) & = g(\xi_i), \quad \text{ on } \partial\Omega, \end{cases} \tag{3.1}$$

where $\{\xi_i = (x_i, y_i)\}_{i=1,\cdots,N} \in \mathcal{D}_{D',\triangle}$ are the domain points of $\triangle$ of degree D as explained in (2.1) in the previous section. Using these points, we have the following matrix equation:

$$-K\mathbf{c} := \left[-\Delta(B^t_{ijk}(\xi_i))\right]\mathbf{c} = [f(\xi_i)] = \mathbf{f},$$

where $\mathbf{c}$ is the vector consisting of all spline coefficients $c^t_{ijk}, i + j + k = D, t \in \triangle$. In general, the spline s with coefficients in $\mathbf{c}$ is a discontinuous function. In order to make $s \in \mathcal{S}^r_D$, its coefficient vector $\mathbf{c}$ must satisfy the constraints $H\mathbf{c} = 0$ for the smoothness conditions that the $\mathcal{S}^r_D$ functions possess (cf. [10]). Our collocation method is to find $\mathbf{c}^*$ by solving the following constrained minimization:

$$\min_{\mathbf{c}} J(c) = \frac{1}{2}(\|B\mathbf{c} - \mathbf{g}\|^2 + \|H\mathbf{c}\|^2) \quad \text{subject to } -K\mathbf{c} = \mathbf{f}, \tag{3.2}$$

where $B, \mathbf{g}$ are from the boundary condition and H is from the smoothness condition. Note that we need to justify that the minimization has a solution. In general, we do not know if the matrix K is invertible and hence, $-K\mathbf{c} = \mathbf{f}$ may not have a solution. However, we can show that a neighborhood of $-K\mathbf{c} = \mathbf{f}$, i.e.

$$\mathbb{N} = \{\mathbf{c} : || - K\mathbf{c} - \mathbf{f}|| \le \epsilon, ||H\mathbf{c}|| \le \epsilon, ||B\mathbf{c} - \mathbf{g}|| \le \epsilon\} \tag{3.3}$$

is not empty.

Indeed, by Lemma 2.1 in the previous section, for any given $\epsilon_1 > 0$, we can find a quasi-interpolatory spline s_u satisfying

$$||\Delta u - \Delta s_u||_\infty \le ||u_{xx} - (s_u)_{xx}||_\infty + ||u_{yy} - (s_u)_{yy}||_\infty \le 2C|\triangle|^{k-2} \le \epsilon_1.$$

if $|\triangle|$ is small enough and $k = D$ is large enough. In other words, at the domain points over $\triangle$ with degree $D' \ge k$, quasi-interpolatory spline s_u from Lemma 2.1 satisfies $| - f(x_i, y_i) - \Delta I(s_u)(x_i, y_i)| = | - f(x_i, y_i) - \Delta s_u(x_i, y_i)| \le \epsilon_1$ for all $1 \le i \le N$. That is, the neighborhood $\mathbb{N}$ in (3.3) is not empty.

We thus consider a nearby problem of the minimization (3.2), that is,

$$\min_c \|B\mathbf{c} - \mathbf{g}\|^2 + ||Hc||^2 \quad \text{subject to} \quad || - K\mathbf{c} - \mathbf{f}||_{L^\infty} \le \epsilon_1. \tag{3.4}$$

It is easy to see that the minimizer of the above (3.4) clearly approximates the minimizer of (3.2).

Next, let $\mathbf{c}^*$ be the minimizer of (3.4) and u_s be the spline with the coefficient vector $\mathbf{c}^*$. Then, we want to prove that our numerical solution u_s is close to the solution u, e.g. $||u - u_s||_{L_2(\Omega)}$ is very small. To describe how small it is, we let $\epsilon_2 = \|B\mathbf{c}^* - \mathbf{g}\|^2 + \|H\mathbf{c}^*\|^2 \geq \|B\mathbf{c}^* - \mathbf{g}\|^2$. That is, $\sum_{(x_i,y_i)\in\partial\Omega} |u(x_i, y_i) - u_s(x_i, y_i)|^2 \leq \epsilon_2$. Without loss of generality, we may assume that u_s approximates u on $\partial\Omega$ very well in the sense that $\|u(x, y) - u_s(x, y)\|_{L^2(\partial\Omega)} \leq C\epsilon_2$ for a positive constant C. Similarly, if the number of collocation points is enough, we have $\|\Delta u_s + f||_{L^2(\Omega)} \leq C\epsilon_1$. We would like to show

$$\|u - u_s\|_{L^2(\Omega)} \leq C|\triangle|^2(\epsilon_1 + \epsilon_2) \tag{3.5}$$

for some constant $C > 0$, where $|\triangle|$ is the size of the underlying triangulation or tetrahedralization $\triangle$ of the domain Ω. To do so, we first show

Lemma 3.1. *Suppose that Ω is a polygonal domain. Suppose that $u \in H^3(\Omega)$. Then there exists a positive constant $\hat{C}$ depending on $D \geq 1$ such that*

$$||\Delta u(x, y) - \Delta u_s(x, y)||_{L^2(\Omega)} \leq \epsilon_1\hat{C}.$$

Proof. Indeed, by Lemma 2.1, we have a quasi-interpolatory spline s_u satisfying

$$|\Delta u(x, y) - \Delta s_u(x, y)| \leq \epsilon_1, \forall(x, y) \in \Omega.$$

Then, we use the minimization (3.4) to have the minimizer u_s satisfying

$$|\Delta u(x_i, y_i) - \Delta u_s(x_i, y_i)| \leq \epsilon_1$$

for any domain points (x_i, y_i) which construct the collocation matrix K. Now, these two inequalities imply that

$$|\Delta u_s(x_i, y_i) - \Delta s_u(x_i, y_i)| \leq \epsilon_1 + \epsilon_1.$$

Note that $\Delta u_s - \Delta s_u$ is a polynomial over each triangle $t \in \triangle$ which has small values at the domain points. This implies that the polynomial $\Delta u_s - \Delta s_u$ is small over t. That is,

$$|\Delta u_s(x, y) - \Delta s_u(x, y)| \leq C(\epsilon_1 + \epsilon_1) = 2C\epsilon_1 \tag{3.6}$$

by using Theorem 2.27 in [10]. Finally, we can use (3.6) to prove

$$|\Delta u(x, y) - \Delta u_s(x, y)| = |\Delta u(x, y) - \Delta s_u(x, y) + \Delta s_u(x, y) - \Delta u_s(x, y)| \leq \epsilon_1 + 2C\epsilon_1.$$

and then

$$||\Delta u(x, y) - \Delta u_s(x, y)||_{L^2(\Omega)} \leq \epsilon_1\hat{C}$$

for a constant $\hat{C}$ depending on the bounded domain Ω and D, D', but independent of $|\triangle|$. ∎

Recall a standard norm on $H^2(\Omega)$ defined in (1.3). In addition, let us define a new norm $\|u\|_L$ on $H^2(\Omega)$ as follows.

$$\|u\|_L = \|\Delta u\|_{L^2(\Omega)} + \|u\|_{L^2(\partial\Omega)} \tag{3.7}$$

We can show that $\|\cdot\|_L$ is a norm on $H^2(\Omega)$ as follows: Indeed, if $\|u\|_L = 0$, then $\Delta u = 0$ in Ω and $u = 0$ on the boundary $\partial\Omega$. By the Green theorem, we get

$$\int_\Omega |\nabla u|^2 = -\int_\Omega u\Delta u + \int_{\partial\Omega} u\frac{\partial u}{\partial n} = 0.$$

This manuscript is for review purposes only.

By Poincaré's inequality, we get

$$||u||_{L^2(\Omega)} \leq C||\nabla u||_{L^2(\Omega)} = 0.$$

Hence, we know that $u = 0$. Next for any scalar a, it is trivial to have $\|au\|_L = \|\Delta au\|_{L^2(\Omega)} + \|au\|_{L^2(\partial\Omega)} = |a|(\|\Delta u\|^2_{L^2(\Omega)} + \|u\|_{L^2(\partial\Omega)})$. Finally, the triangular inequality is also trivial.

$$\|u+v\|_L = \|\Delta(u+v)\|_{L^2(\Omega)} + \|u+v\|_{L^2(\partial\Omega)} \leq \|u\|_L + \|v\|_L$$

by linearity of the Laplacian operator.

We now show that the new norm is equivalent to the standard norm on $H^2(\Omega)$. Indeed, recall a well-known property about the norm equivalence.

LEMMA 3.2. *([Brezis, 2011 [2]]) Let E be a vector space equipped with two norms, $\|\cdot\|_1$ and $\|\cdot\|_2$. Assume that E is a Banach space for both norms and that there exists a constant $C > 0$ such that*

$$\|x\|_2 \leq C\|x\|_1, \ \forall x \in E. \tag{3.8}$$

Then the two norms are equivalent, i.e., there is a constant $c > 0$ such that

$$\|x\|_1 \leq c_1\|x\|_2, \ \forall x \in E.$$

Proof. We define $E_1 = (E, ||\cdot||_1)$ and $E_2 = (E, ||\cdot||_2)$ be two spaces equipped with two different norms. It is easy to see that E_1 and E_2 are Banach spaces. Let I be the identity operator which maps any u in E_1 to u in E_2. Clearly, it is an injection and onto because of the identity mapping and hence, it is a surjection. Because of (3.8), the mapping I is a continuous operator. Now we can use the well-known open mapping theorem. Let $B_1(0,1) = \{u \in E_1, ||u||_1 \leq 1\}$ be an open ball. The open mapping theorem says that $I(B_1(0,1))$ is open and hence, it contains a ball $B_2(0,c) = \{u \in E_2, ||u||_2 < c\}$. That is, $B_2(0,c) \subset I(B_1(0,1))$. Let us claim that $c||u||_1 \leq ||I(u)||_2$ for all $u \in E_1$. Otherwise, there exists a u^* such that $c||u^*||_1 > ||I(u^*)||_2$. That is, $c > ||I(u^*/||u^*||_1)||_2$. So $I(u^*/||u^*||_1) \in B_2(0,c)$. There is a $u^{**} \in B_1(0,1)$ such that $Iu^{**} = I(u^*/||u^*||_1)$. Since I is an injection, $u^{**} = I(u^*/||u^*||_1$. Since $u^{**} \in B_1(0,1)$, we have $1 > ||u^{**}||_1 = ||(u^*/||u^*||_1))\| = 1$ which is a contradiction. This shows that the claim is correct. we have thus $c||u||_1 \leq ||I(u)||_2 = ||u||_2$ for all $u \in E_1$. We choose $c_1 = 1/c$ to finish the proof. ∎

THEOREM 3.3. *Suppose $\Omega \subset \mathbb{R}^d$ is a multiple-strictly-star-shaped domain, e.g. a polygonal domain. There exist two positive constants A and B such that*

$$A\|u\|_{H^2} \leq \|u\|_L \leq B\|u\|_{H^2}, \quad \forall u \in H^2(\Omega). \tag{3.9}$$

Proof. We first use the trace Theorem 2.5 from the previous section. Mainly we shall use the inequality in (2.2). It then follows that

$$\begin{aligned} \|u\|_L &\leq \|\Delta u\|_{L^2(\Omega)} + \|u\|_{L^2((\partial\Omega)} \\ &\leq \sum_{i,j=1}^d \|\frac{\partial^2}{\partial x_i \partial x_j} u\|_{L^2(\Omega)} + C(\|u\|_{L^2(\Omega)} + \|\nabla u\|_{L^2(\Omega)}) \leq B\|u\|_{H^2} \end{aligned} \tag{3.10}$$

for all $u \in H^2(\Omega)$, where $B = \max\{1, C\}$. We then use Lemma 3.2 to finish the proof. Indeed, by Lemma 3.2 and the above inequality, there exist $\alpha > 0$ satisfying

$$\|u\|_{H^2} \leq \alpha\|u\|_L.$$

Therefore, we choose $A = \frac{1}{\alpha}$ to finish the proof. ∎

Using Theorem 3.3, we immediately obtain the following theorem

THEOREM 3.4. *Suppose f and g are continuous over bounded domain $\Omega \subseteq \mathbb{R}^d$ for $d \geq 2$. Suppose that $u \in H^3(\Omega)$. When Ω is a multiple-strictly-star-shaped domain or a polygon, we have the following inequality*

$$||u - u_s||_{L^2(\Omega)} \leq C(\epsilon_1 + \epsilon_2), ||\nabla(u - u_s)||_{L^2(\Omega)} \leq C(\epsilon_1 + \epsilon_2)$$

and

$$\sum_{i+j=2} \|\frac{\partial^2}{\partial x^i \partial y^j} u\|_{L^2(\Omega)} \leq C(\epsilon_1 + \epsilon_2)$$

for a positive constant C depending on A and Ω, where A is one of the constants in Theorem 3.3.

Proof. Using Lemma 3.1 and the assumption on the approximation on the boundary, we have

$$||u - u_s||_{H^2(\Omega)} \leq \frac{1}{A}(\|\Delta(u - u_s)\|_{L^2(\Omega)} + \|u - u_s\|_{L^2(\partial\Omega)}) \leq \frac{1}{A}(\epsilon_1 \hat{C} + \epsilon_2 C_{\partial\Omega})$$

where $C_{\partial\Omega}$ denotes the length of the boundary of Ω. We choose $C = \frac{\max\{\hat{C}, C_{\partial\Omega}\}}{A}$ to finish the proof. ∎

Finally we show that the convergence of $\|u - u_s\|_{L^2(\Omega)}$ and $\|\nabla(u - u_s)\|_{L^2(\Omega)}$ can be better

THEOREM 3.5. *Suppose that $(u - u_s)|_{\partial\Omega} = 0$. Under the assumptions in Theorem 3.4, we have the following inequality*

$$||u - u_s||_{L^2(\Omega)} \leq C|\triangle|^2(\epsilon_1 + \epsilon_2) \text{ and } ||\nabla(u - u_s)||_{L^2(\Omega)} \leq C|\triangle|(\epsilon_1 + \epsilon_2)$$

for a positive constant $C = 1/A$, where A is one of the constants in Theorem 3.3 and $|\triangle|$ is the size of the underlying triangulation $\triangle$.

Proof. First of all, it is known for any $w \in H^2(\Omega)$, there is a continuous linear spline L_w over the triangulation $\triangle$ such that

$$\|D_x^\alpha D_y^\beta (w - L_w)\|_{L^2(\Omega)} \leq C|\triangle|^{2-\alpha-\beta}|w|_{H^2(\Omega)} \tag{3.11}$$

for nonnegative integers $\alpha \geq 0, \beta \geq 0$ and $\alpha+\beta \leq 2$, where $|w|_{H^2(\Omega)}$ is the semi-norm of w in $H^2(\Omega)$. Indeed, we can use the same construction method for quasi-interpolatory splines used for the proof of Lemma 2.1 to establish the above estimate. The above estimate will be used twice below.

By the assumption that $u - u_s = 0$ on $\partial\Omega$, it is easy to see

$$\begin{aligned}
&\|\nabla(u - u_s)\|^2_{L^2(\Omega)} = -\int_\Omega \Delta(u - u_s)(u - u_s) = -\int_\Omega \Delta(u - u_s - L_{u-u_s})(u - u_s) \\
&= \int_\Omega \nabla(u - u_s - L_{u-u_s})\nabla(u - u_s) \leq \|\nabla(u - u_s)\|_{L^2(\Omega)}\|\nabla(u - u_s - L_{u-u_s})\|_{L^2(\Omega)} \\
&\leq \|\nabla(u - u_s)\|_{L^2(\Omega)} C|\triangle| \cdot |u - u_s|_{H^2(\Omega)} \\
&\leq \|\nabla(u - u_s)\|_{L^2(\Omega)}|\triangle|\frac{C}{A}\|\Delta(u - u_s)\|_{L^2(\Omega)}.
\end{aligned}$$

where we have used the first inequality in Theorem 3.3. It follows that $\|\nabla(u - u_s)\|^2_{L^2(\Omega)} \leq |\triangle|\frac{C}{A}(\epsilon_1 + \epsilon_2)$.

Next we let $w \in H^2(\Omega)$ be the solution to the following Poisson equation:

$$\begin{cases} -\Delta w &= u - u_s \quad \text{in } \Omega \subset \mathbb{R}^d \\ \quad w &= 0 \quad \text{on } \partial\Omega, \end{cases} \tag{3.12}$$

Then we use the continuous linear spline L_w to have

$$\begin{aligned} \|(u-u_s)\|^2_{L^2(\Omega)} &= -\int_\Omega \Delta w(u-u_s) = -\int_\Omega \Delta(w-L_w)(u-u_s) \\ &= \int_\Omega \nabla(w-L_w)\nabla(u-u_s) \le \|\nabla(u-u_s)\|_{L^2(\Omega)}\|\nabla(w-L_w)\|_{L^2(\Omega)} \\ &\le \|\nabla(u-u_s)\|_{L^2(\Omega)} C|\triangle|\cdot|w|_{H^2(\Omega)} \le \frac{C}{A}|\triangle|(\epsilon_1+\epsilon_2)|\triangle|\frac{C}{A}\|\Delta w\|_{L^2(\Omega)} \\ &= \frac{C}{A}|\triangle|(\epsilon_1+\epsilon_2)|\triangle|\frac{C}{A}\|u-u_s\|_{L^2(\Omega)}. \end{aligned}$$

where we have used the first inequality in Theorem 3.3 and the estimate of $\|\nabla(u-u_s)\|_{L^2(\Omega)}$ above. Hence, we have $\|(u-u_s)\|^2_{L^2(\Omega)} \le \frac{C^2}{A^2}|\triangle|^2(\epsilon_1+\epsilon_2)$ as $|\triangle| \to 0$. ∎

4. General Second Order Elliptic Equations. Now we consider a collocation method based on bivariate/trivariate splines for a solution of the general second order elliptic equation in (1.2). For the PDE coefficient functions $a^{ij}, b^i, c^1 \in L^\infty(\Omega)$, we assume that

$$a_{ij} = a_{ji} \in L^\infty(\Omega) \quad \forall i, j =, \cdots, d \tag{4.1}$$

and there exist λ, Λ such that

$$\lambda \sum_{i=1}^d \eta_i^2 \le \sum_{i,j}^d a^{ij}(x)\eta_i\eta_j \le \Lambda \sum_{i=1}^d \eta_i^2, \forall \eta \in \mathbb{R}^d \backslash \{0\} \tag{4.2}$$

for all i, j and $x \in \Omega$. For convenience, we first assume that $b^i \equiv 0$ and $c^1 = 0$. In addition to the elliptic condition, we add the Cordés condition for well-posedness of the problem. We assume that there is an $\epsilon \in (0,1]$ such that

$$\frac{\sum_{i,j=1}^d (a^{i,j})^2}{(\sum_{i=1}^d a^{ii})^2} \le \frac{1}{d-1+\epsilon} \quad \textit{a.e. in } \Omega \tag{4.3}$$

Let $\gamma \in L^\infty(\Omega)$ be defined by

$$\gamma := \frac{\sum_{i=1}^d a^{ii}}{\sum_{i,j=1}^d (a^{i,j})^2}.$$

Under these conditions, the researchers in [18] proved the following lemma

LEMMA 4.1. *Let the operator $\mathcal{L}_1(u) := \sum_{i,j=1}^d a^{ij}(x)\frac{\partial^2}{\partial x_i \partial x_j} u$ satisfy (4.1), (4.2) and (4.3). Then for any open set $U \subseteq \Omega$ and $v \in H^2(U)$, we have*

$$|\gamma \mathcal{L}_1 v - \Delta v| \le \sqrt{1-\epsilon}|D^2 v| \quad \textit{a.e. in } U, \tag{4.4}$$

where $\epsilon \in (0,1]$ is as in (4.3).

Instead of using the convexity to ensure the existence of the strong solution of (1.2) in [18], we shall use the concept of uniformly positive reach in [5]. The following is just the restatement of Theorem 3.3 in [5].

THEOREM 4.2. *Suppose that $\Omega \subset \mathbb{R}^d$ with $d \geq 2$ is a bounded domain with uniformly positive reach. Then the second order elliptic PDE in (1.2) satisfying (4.3) has a unique strong solution in $H^2(\Omega)$.*

We now extend the collocation method in the previous section to find a numerical solution of (1.2). Similar to the discussion in the previous section, we can construct the following matrix for the PDE in (1.2):

$$\mathcal{K} = \mathbf{a}_{11} MxxV + (\mathbf{a}_{12} + \mathbf{a}_{21}) MxyV + \mathbf{a}_{22} MyyV,$$

where $\mathbf{a}_{11}$ is the vector of the PDE coefficient $a^{11}(\xi_i), i = 1, \cdots, N$ and similar for other vectors. Similar to (3.4), consider the following minimization problem:

$$\min_{\mathbf{c}} J(c) = \frac{1}{2}(\|B\mathbf{c} - \mathbf{g}\|^2 + \|H\mathbf{c}\|^2) \quad \text{subject to } -\mathcal{K}\mathbf{c} = \mathbf{f}, \tag{4.5}$$

Again we will solve a nearby minimization problem as in the previous section. Just like the Poisson equation, we let $\epsilon_1 = \|\mathcal{K}\mathbf{c}^* + \mathbf{f}\|_\infty$ and $\epsilon_2 = \|B\mathbf{c} - \mathbf{g}\|^2 + \|H\mathbf{c}\|^2 \geq \|B\mathbf{c} - \mathbf{g}\|^2$ be the minimal value of (4.5). In fact, we may assume that the solution u_s for (4.5) approximates u very well in the sense that $\|u - u_s\|_{L^2(\partial\Omega)} \leq \epsilon_2$ and $\|\mathcal{L}u_s + f\|_{L^2(\Omega)} \leq \epsilon_1$.

To show u_s approximate u over Ω, let us define a new norm $\|u\|_{\mathcal{L}}$ on $H^2(\Omega)$ as follows.

$$\|u\|_{\mathcal{L}} = \|\mathcal{L}u\|_{L^2(\Omega)} + \|u\|_{L^2(\partial\Omega)} \tag{4.6}$$

We can show that $\|\cdot\|_{\mathcal{L}}$ is a norm on $H^2(\Omega)$ as follows if $\epsilon \in (0,1]$ is large enough. Indeed, if $\|u\|_{\mathcal{L}} = 0$, then $\mathcal{L}u = 0$ in Ω and $u = 0$ on the boundary $\partial\Omega$. Using this Lemma 4.1 and Theorem 3.3, we get

$$\int_\Omega \Delta u \Delta u - \int_\Omega (\Delta - \gamma\mathcal{L}) u \Delta u = \int_\Omega \gamma\mathcal{L}(u)\Delta u = 0 \tag{4.7}$$

and

$$\begin{aligned}\int_\Omega \Delta u \Delta u - \int_\Omega (\Delta - \gamma\mathcal{L}) u \Delta u &\geq \int_\Omega |\Delta u|^2 - \int_\Omega \sqrt{1-\epsilon}|D^2 u| \cdot |\Delta u| \\ &= \int_\Omega |\Delta u|^2 - \int_\Omega \sqrt{1-\epsilon}|D^2 u| \cdot |\Delta u| \geq \|\Delta u\|^2 - \frac{\sqrt{1-\epsilon}}{A}\|\Delta u\|\|\Delta u\|\end{aligned}$$

Therefore, if $\epsilon > 1 - A^2$, then

$$(1 - \frac{\sqrt{1-\epsilon}}{A})\|\Delta u\| \leq 0.$$

Hence, we know that $u = 0$. The other two properties of the norm can be proved easily. We mainly show that the above norm is equivalent to the standard norm on $H^2(\Omega)$.

THEOREM 4.3. *Suppose that Ω has uniformly positive reach $r_\Omega > 0$ and is a multiple-strictly-star-shaped domain. Then there exist two positive constants A_1 and B_1 such that*

$$A_1\|u\|_{H^2(\Omega)} \leq \|u\|_{\mathcal{L}} \leq B_1\|u\|_{H^2(\Omega)}, \quad \forall u \in H^2(\Omega). \tag{4.8}$$

Proof. We first use the trace theorem 2.5 that

$$\|u\|_{L^2(\partial\Omega)} \leq C(\|u\|_{L^2(\Omega)} + \|\nabla u\|_{L^2(\Omega)})$$

for $u \in H^1(\Omega)$. It follows that

$$\|u\|_{\mathcal{L}} \leq \max_{i,j=1\cdots,d} \|a^{ij}\|_\infty \sum_{i,j=1}^{d} \|\frac{\partial^2}{\partial x_i \partial x_j} u\|_{L^2(\Omega)} + C\|\nabla u\|_{L^2(\Omega)} + C\|u\|_{L^2(\Omega)} \leq B_1 \|u\|_{H^2(\Omega)}$$

for all $u \in H^2(\Omega)$, where B_1 depending on d, Λ and C. Using Lemma 4 and the above inequality, there exist $\alpha_1 > 0$ satisfying

$$\|u\|_{H^2} \leq \alpha_1 \|u\|_{\mathcal{L}}.$$

Therefore, we choose $A_1 = \frac{1}{\alpha_1}$ to finish the proof. ∎

THEOREM 4.4. *Let Ω be a bounded and closed set satisfying the uniformly positive reach condition. Assume that $a^{ij} \in L^\infty(\Omega)$ satisfy (4.1), (4.2) and (4.3) and $\epsilon > 1 - A^2$. Suppose that $u \in H^3(\Omega)$. For the solution u of equation (1.10) and the corresponding minimizer u_s, we have the following inequality*

$$||u - u_s||_{L^2(\Omega)} \leq C(\epsilon_1 + \epsilon_2)$$

for a positive constant C depending on Ω and A_1 which is one of the constants in Theorem 4.3. Similar for $\|\nabla(u - u_s)\|_{L^2(\Omega)}$ and $|u - u_s|_{H^2}$.

Next we consider the case that b^i and c^1 are not zero. Assume that $\|a^{ij}\|_\infty$, $\|b^i\|_\infty$, $\|c^1\|_\infty \leq \Lambda_1$ and we denote that $\mathcal{L}_1(u) := \sum_{i,j=1}^d a^{ij}(x) \frac{\partial^2}{\partial x_i \partial x_j} u + \sum_{i=1}^d b^i(x) \frac{\partial}{\partial x_i} u + c^1(x)u$ and define a new norm $\|u\|_{\mathcal{L}_1}$ on $H^2(\Omega)$ as follows.

$$\|u\|_{\mathcal{L}_1} = \|\mathcal{L}_1 u\|_{L^2(\Omega)} + \|u\|_{L^2(\partial\Omega)}. \tag{4.9}$$

Assume that $\|u\|_{\mathcal{L}_1} = 0$, i.e., $\mathcal{L}_1 u = 0$ over Ω and $u = 0$ on $\partial\Omega$. From (4.4), we have

$$\int_\Omega \gamma \mathcal{L}(u) \Delta u \geq \|\Delta u\|^2 - \frac{\sqrt{1-\epsilon}}{A} \|\Delta u\|^2.$$

Then by the above inequality we get

$$\begin{aligned}
0 &= \int_\Omega \gamma \mathcal{L}_1(u) \Delta u = \int_\Omega \gamma \mathcal{L}(u) \Delta u + \sum_{i=1}^{d} \gamma b^i(x) \frac{\partial}{\partial x_i} u \Delta u + \gamma c^1(x) u \Delta u \\
&\geq \|\Delta u\|^2 - \frac{\sqrt{1-\epsilon}}{A} \|\Delta u\|^2 + \int_\Omega \sum_{i=1}^{d} \gamma b^i(x) \frac{\partial}{\partial x_i} u \Delta u + \gamma c^1(x) u \Delta u \\
&\geq \|\Delta u\|^2_{L^2(\Omega)} - \frac{\sqrt{1-\epsilon}}{A} \|\Delta u\|^2_{L^2(\Omega)} - \|\gamma\|_\infty \max_i \|b^i\|_\infty \sqrt{d} \|\nabla u\|_{L^2(\Omega)} \|\Delta u\|_{L^2(\Omega)} \\
&\quad - \|\gamma\|_\infty \|c^1\|_\infty \|u\|_{L^2(\Omega)} \|\Delta u\|_{L^2(\Omega)} \\
&\geq \|\Delta u\|^2_{L^2(\Omega)} - \frac{\sqrt{1-\epsilon}}{A} \|\Delta u\|^2_{L^2(\Omega)} - C_m(\|\nabla u\|_{L^2(\Omega)} \|\Delta u\|_{L^2(\Omega)} + \|u\|_{L^2(\Omega)} \|\Delta u\|_{L^2(\Omega)})
\end{aligned}$$

where $C_m = \max\{\|\gamma\|_\infty \max_i \|b^i\|_\infty \sqrt{d}, \|\gamma\|_\infty \|c^1\|_\infty\}$. By Poincaré inequality, we have $\|u\|_{L^2(\Omega)} \leq C\|\nabla u\|_{L^2(\Omega)} \leq C^2 \|\Delta u\|_{L^2(\Omega)}$ for some constant C. Using Theorem

3.3, it is followed that

$$0 \geq \|\Delta u\|_{L^2(\Omega)} - \frac{\sqrt{1-\epsilon}}{A}\|\Delta u\|_{L^2(\Omega)} - C_m(\|\nabla u\|_{L^2(\Omega)} + \|u\|_{L^2(\Omega)})$$
$$\geq \|\Delta u\|_{L^2(\Omega)} - \frac{\sqrt{1-\epsilon}}{A}\|\Delta u\|_{L^2(\Omega)} - C_m(C+C^2)\|u\|_{H^2(\Omega)}$$
$$\geq \|\Delta u\|_{L^2(\Omega)} - \frac{\sqrt{1-\epsilon}}{A}\|\Delta u\|_{L^2(\Omega)} - \frac{C_m(C+C^2)}{A}\|\Delta u\|_{L^2(\Omega)}$$
$$= \|\Delta u\|_{L^2(\Omega)}(1 - \frac{\sqrt{1-\epsilon}}{A} - \frac{C_m(C+C^2)}{A}).$$

If the term $(1 - \frac{\sqrt{1-\epsilon}}{A} - \frac{C_m(C+C^2)}{A})$ is positive, then we can conclude that $\Delta u = 0$. Since $\Delta u = 0$ and $u = 0$ on $\partial\Omega$, $\|u\|_L = 0$ and then $u = 0$. Similar to the proof of other norms $\|\cdot\|_L$ and $\|\cdot\|_{\mathcal{L}}$, it is easy to prove that $\|u+v\|_{\mathcal{L}_1} \leq \|u\|_{\mathcal{L}_1} + \|v\|_{\mathcal{L}_1}$ and $\|au\|_{\mathcal{L}_1} = |a|\|u\|_{\mathcal{L}_1}$. The detail is omitted.

THEOREM 4.5. *Assume that* $(1 - \frac{\sqrt{1-\epsilon}}{A} - \frac{C_m(C+C^2)}{A}) > 0$. *There exist two positive constants* A_2 *and* B_2 *such that*

$$A_2\|u\|_{H^2(\Omega)} \leq \|u\|_{\mathcal{L}} \leq B_2\|u\|_{H^2(\Omega)}, \quad \forall u \in H^2(\Omega). \tag{4.10}$$

Proof. The proof is similar to before. We leave it to the interested reader. ∎

Therefore, we can get the following theorem for the general elliptic PDE:

THEOREM 4.6. *Let* Ω *be a multiple-strictly-star-shaped domain and has a uniformly positive reach. Assume that* $a^{ij}, b^i, c^1 \in L^\infty(\Omega)$ *satisfy* (4.1), (4.2), (4.3) *and* $(1 - \frac{\sqrt{1-\epsilon}}{A} - \frac{C_m(C+C^2)}{A}) > 0$. *Suppose that* $u \in H^3(\Omega)$. *For the solution* u *of equation* (1.2) *and the corresponding minimizer* u_s, *we have the following inequality*

$$||u - u_s||_{L^2(\Omega)} \leq C(\epsilon_1 + \epsilon_2)$$

for a positive constant C *depending on* Ω *and a constant* A_2 *in Theorem 4.5.*

Finally we show that the convergence of $\|u - u_s\|_{L^2(\Omega)}$ and $\|\nabla(u - u_s)\|_{L^2(\Omega)}$ can be better

THEOREM 4.7. *Suppose that the bounded domain* Ω *has an uniformly positive reach. Suppose* f *and* g *are continuous over bounded domain* $\Omega \subseteq \mathbb{R}^d$ *for* $d = 2, 3$. *Suppose that* $u \in H^3(\Omega)$. *If* $u - u_s|_{\partial\Omega} = 0$, *we further have the following inequality*

$$||u - u_s||_{L^2(\Omega)} \leq C|\triangle|^2(\epsilon_1 + \epsilon_2) \text{ and } ||\nabla(u - u_s)||_{L^2(\Omega)} \leq C|\triangle|(\epsilon_1 + \epsilon_2)$$

for a positive constant $C = 1/A_2$, *where* A_2 *is one of the constants in Theorem 3.3 and* $|\triangle|$ *is the size of the underlying triangulation* $\triangle$.

Proof. The proof is similar to Theorem 3.5. We leave the detail to the interested reader. ∎

5. Implementation of the Spline based Collocation Method. Before we present our computational results for Poisson equation and general second order elliptic equations, let us first explain the implementation of our spline based collocation method. We divide the implementation into two parts. The first part of the implementation is to construct the collocation matrices K and $\mathcal{K}$ associated with the triangulation/tetrahedralization, the degree D of spline functions and the smoothness

$r \geq 1$ as well as the domain points associated with the triangulation/tetrahedralization and degree D'. This part also generates the smoothness matrix H. More precisely, for the Poisson equation, we construct $MxxV := [(B^t_{ijk}(\mathbf{x})_{xx}|_{\mathbf{x}=\xi_\ell}]$ and $MyyV := [(B^t_{ijk}(\mathbf{x})_{yy}|_{\mathbf{x}=\xi_\ell}]$. In fact we choose many other points which are in addition to the domain points to build these $MxxV$ and $MyyV$. Then $K = MxxV + MyyV$ is a size of $2m \times m$ for the Poisson equation, where $m = \dim(S^{-1}_D(\triangle))$. After generating matrices, we save our matrices which will be used later for solution of the Poisson equation for various right-hand side functions and boundary conditions. And, for the general elliptic equations, we first generate all the related matrices $MxxV, MxyV, MyyV, MxV, MyV, \cdots$ as the same as for the Poisson equation. Then we generate the collocation matrix $\mathcal{K}$ associated with the PDE coefficients at the same domain points as well as the additional points from all the related matrices $MxxV, MxyV, MyyV, MxV, MyV, \cdots$ which are already generated before. This part is the most time consumed step. See Tables 1 and 2 for the 2D and 3D settings.

The second part, Part 2 is to construct the right-hand side vector $\mathbf{f}$ and the matrix B and vector G associated with the boundary condition as well as use an iterative method which is similar to [1] to solve the minimization problem (3.4) and (4.5). See Table 3 for computational times for the 3D setting.

We shall use the four different domains in 2D shown in Fig. 1 and four different domains in 3D shown in Fig. 2 to test the performance of our collocation method. In addition, the spline based collocation method has been tested over many more domains of interest. Numerical results can be found in [14].

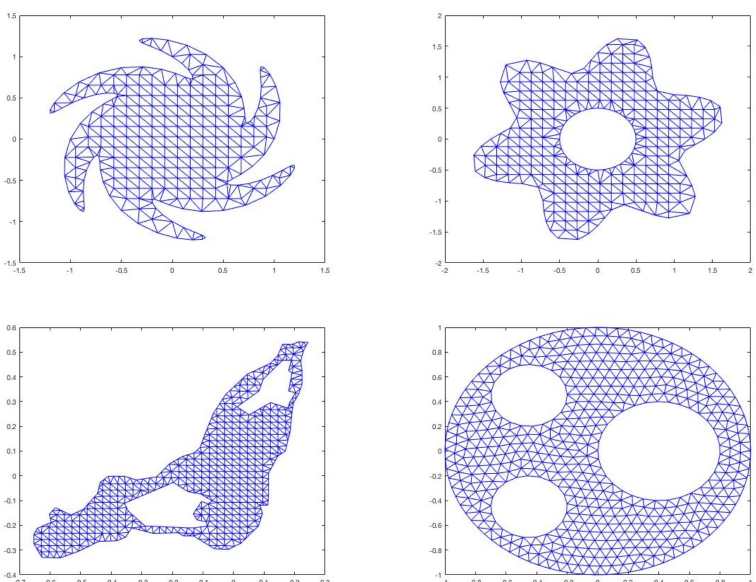

FIG. 1. *Several domains in $\mathbb{R}^2$ used for Numerical Experiments*

In our computational experiments, we use a cluster computer at University of Georgia to generate the related collocation matrices for various degree of splines and domain points as described in the part I. We use multiple CPUs in the computer so that multiple operations can be done simultaneously. For the 2D case, we use 2 processors on a parallel computer, which has 1.8GHz Intel Core i5 processors for Part 1

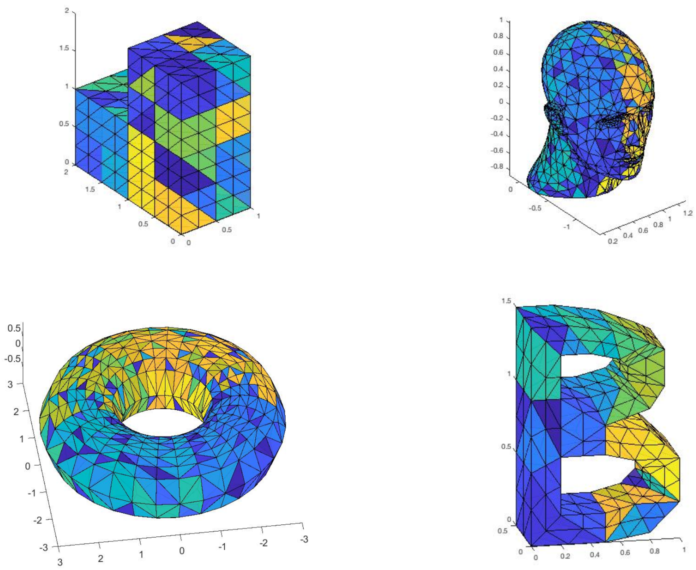

FIG. 2. *Several 3D domains used for Numerical Experiments*

Domains	Number of vertices	Number of triangles	degree	Time (P)	Time (G)	Time (UGA P)	Time (UGA G)
Gear	274	426	8	5.27e+01	3.31e+02	2.98e+01	3.49e+01
Flower	297	494	8	5.83e+01	4.09e+02	3.32e+01	4.20e+01
Montreal	549	870	8	9.83e+01	7.26e+02	2.95e+01	8.55e+01
Circle	525	895	8	1.18e+02	1.19e+03	2.78e+01	8.40e+01

TABLE 1
Times in seconds for generating necessary matrices for each 2D domain in Figure 1.

and Part 2. And we also use a high memory (512GB) node from the Sapelo 2 cluster at University of Georgia, which has four AMD Opteron 6344 2.6 GHz processors. Using 48 processors on the UGA cluster, we can generate our necessary matrices and the computational times for Part 1 are listed in Table 1. For 3D case, we use 48 processors for Part 1 and 12 processors for Part 2 to do the computation. Tables 2 and 3 show the computational times for generating collocation matrices, where (P), (UGA P) indicates the time for the Poisson equation with 2 processors and 48 processors respectively and (G), (UGA G) for the general second order PDE using 2 processors and 48 processors, respectively.

6. Numerical results for the Poisson Equation. We shall present computational results for 2D Poisson equation and 3D Poisson equations separately in the following two subsections. In each section, we first present the computational results from the spline based collocation method to demonstrate the accuracy the method can achieve. Then we present a comparison of our collocation method with the numerical method proposed in [1] which uses multivariate splines to find the weak solution like finite element method. For convenience, we shall call our spline based collocation method the LL method and the numerical method in [1] the AWL method.

6.1. Numerical examples for 2D Poisson equations. We have used various triangulations over various bounded domains as shown in [14] and tested many solu-

Domains	Number of vertices	Number of tetrahedron	Degree of splines	Time (UGA P)	Time (UGA G)
L-shaped domain	325	1152	9	3.71e+03	4.785e+03
Human head	913	1588	9	6.62e+03	8.278e+03
Torus	773	2911	9	9.55e+03	1.180e+04
Letter B	299	816	9	1.71e+03	2.347e+03

TABLE 2

Times in seconds for generating necessary matrices for each 3D domain in Figure 2.

Domain	Time (P)	Time (SG)	Time (NSG1)	Time (NSG2)
L shaped domain	1.0729e+02	2.8400e+02	9.6750e+01	6.2362e+01
Human head	9.6791e+01	2.2425e+02	1.0746e+02	5.7200e+01
Torus	4.5197e+02	6.3574e+02	3.2542e+02	2.2183e+02
Letter B	3.7484e+01	9.6532e+01	1.5394e+02	2.2085e+01

TABLE 3

Times in seconds for finding solutions of 3D Poisson equation(P), general second order elliptic equation with smooth PDE coefficients (SG) or with non-smooth PDE coefficients (NSG1, NSG2) for each domain in Figure 2.

tions to the Poisson equation to see the accuracy that the LL method can do. For convenience, we shall only present a few of the computational results based on the domains in Figure 1. The following is a list of 10 testing functions (8 smooth solutions and 2 not very smooth)

$$
\begin{aligned}
u^{s1} &= e^{\frac{(x^2+y^2)}{2}},\\
u^{s2} &= \cos(xy) + \cos(\pi(x^2+y^2)),\\
u^{s3} &= \frac{1}{1+x^2+y^2},\\
u^{s4} &= \sin(\pi(x^2+y^2)) + 1,\\
u^{s5} &= \sin(3\pi x)\sin(3\pi y),\\
u^{s6} &= \arctan(x^2-y^2),\\
u^{s7} &= -\cos(x)\cos(y)e^{-(x-\pi)^2-(y-\pi)^2}\\
u^{s8} &= \tanh(20y-20x^2) - \tanh(20x-20y^2),\\
u^{ns1} &= |x^2+y^2|^{0.8} \text{ and}\\
u^{ns2} &= (xe^{1-|x|}-x)(ye^{1-|y|}-y).
\end{aligned}
$$

Note that the test function in u^{s8} is notoriously difficult to compute. One has to use a good adaptive triangulation method (cf. [9]). The maximum errors, root mean squared error(RMSE) of approximate spline solutions against the exact solution are given in Table 4. These errors are computed based on 501×501 equally-spaced points fell inside the different domains in Figure 1. We chose collocation points to create $2m\times m$ matrix K, where m is the number of Bernstein basis functions (the dimension of spline space $S_D^{-1}(\triangle)$) and used an iterative method similar to the one in [1] to find the numerical solutions.

From Table 4, we can see that the performance of our method is excellent. Next let us compare with the numerical method in [1] for the same degree, the same smoothness, and the same triangulation. The comparison results are shown in Table 5. One can see that both methods perform very well. Our method can achieve a better accuracy due to the reason the more number of collocation points is used than the dimension of spline space $S_D^{-1}(\triangle)$.

Finally, we summarize the computational times for both methods in Table 6. One can see the LL method can be more efficient if the collocation matrices are already

	Gear		Flower with a hole		Montreal		Circle with 3 holes	
Solution	RMSE	error	RMSE	error	RMSE	error	RMSE	error
u^{s1}	1.40e-10	3.43e-10	9.33e-12	4.04e-11	8.03e-11	2.45e-10	2.95e-12	1.08e-11
u^{s2}	1.30e-09	1.06e-08	1.54e-07	7.88e-07	1.29e-10	4.20e-10	4.33e-12	1.13e-11
u^{s3}	6.03e-11	1.87e-10	9.01e-12	3.25e-11	1.05e-10	3.09e-10	1.90e-12	5.43e-12
u^{s4}	1.20e-09	6.15e-09	1.20e-07	7.88e-07	1.15e-10	2.99e-10	7.44e-12	2.23e-11
u^{s5}	3.82e-07	2.36e-06	5.87e-06	2.40e-05	2.04e-11	5.40e-11	3.40e-10	1.16e-09
u^{s6}	6.13e-10	1.32e-08	8.73e-08	5.93e-07	1.86e-12	6.71e-12	1.09e-12	4.10e-12
u^{s7}	1.44e-11	3.42e-11	7.05e-13	1.64e-12	1.51e-11	4.25e-11	1.51e-13	5.74e-13
u^{s8}	5.71e-02	2.61e-01	5.22e-01	2.32e+00	1.53e-08	3.44e-07	3.00e-04	4.01e-03
u^{ns1}	1.81e-05	1.34e-03	3.97e-11	2.17e-10	1.33e-05	1.80e-04	2.36e-05	3.36e-04
u^{ns2}	1.71e-04	7.29e-04	1.33e-04	8.41e-04	3.58e-06	2.02e-05	1.39e-05	1.58e-04

Table 4

The RMSE and the maximum errors of spline solutions for Poisson equations from the matrix iterative method over several domains when $r = 2$ and $D = 8$.

	Gear		Flower with a hole		Montreal		Circle with 3 holes	
Sol'n	AWL	LL	AWL	LL	AWL	LL	AWL	LL
u^{s1}	1.40e-05	3.43e-10	3.27e-05	4.04e-11	8.89e-07	2.45e-10	3.28e-06	1.08e-11
u^{s2}	6.41e-05	1.06e-08	8.52e-05	7.88e-07	3.48e-06	4.20e-10	2.02e-06	1.13e-11
u^{s3}	8.55e-06	1.87e-10	4.19e-06	3.25e-11	1.03e-06	3.09e-10	1.04e-06	5.43e-12
u^{s4}	2.95e-05	6.15e-09	3.70e-05	7.88e-07	3.63e-06	2.99e-10	1.26e-05	2.23e-11
u^{s5}	1.03e-04	2.36e-06	1.36e-04	2.40e-05	1.70e-05	5.40e-11	3.10e-05	1.16e-09
u^{s6}	3.02e-05	1.32e-08	1.25e-05	5.93e-07	2.06e-06	6.71e-12	5.94e-06	4.10e-12
u^{s7}	1.74e-10	3.42e-11	1.56e-10	1.64e-12	3.11e-07	4.25e-11	1.32e-11	5.74e-13
u^{s8}	1.78e+00	2.61e-01	2.65e+00	2.32e+00	2.42e-06	3.44e-07	5.71e-02	4.01e-03
u^{ns1}	6.53e-03	1.34e-03	1.74e-05	2.17e-10	1.73e-04	1.80e-04	5.39e-03	3.36e-04
u^{ns2}	8.47e-03	7.29e-04	1.44e-03	8.41e-04	1.84e-04	2.02e-05	5.25e-04	1.58e-04

Table 5

The maximum errors of spline solutions for the Poisson equation over the four domains in Figure 1 when $r = 2$ and $D = 8$ for both the AWL method and the LL method.

generated. The LL method can be useful for time dependent PDE such as the heat equation. We only need to generate the collocation matrix once and use it repeatedly for many time step iterations.

6.2. Numerical results for the 3D Poisson equation. We have used our collocation method to solve the 3D Poisson equation and the tested 10 smooth and non-smooth solution over various domains. For convenience, we only show a few computational results to demonstrate that our collocation method works very well. More detail can be found in [14]. Our testing smooth solutions are as follows:

$$\begin{aligned}
u^{3ds1} &= \sin(2x+2y)\tanh(\frac{xz}{2})\\
u^{3ds2} &= e^{\frac{x^2+y^2+z^2}{2}}\\
u^{3ds3} &= \cos(xyz)+\cos(\pi(x^2+y^2+z^2))\\
u^{3ds4} &= \frac{1}{1+x^2+y^2+z^2}\\
u^{3ds5} &= \sin(\pi(x^2+y^2+z^2))+1\\
u^{3ds6} &= 10e^{-x^2-y^2-z^2}\\
u^{3ds7} &= \sin(2\pi x)\sin(2\pi y)\sin(2\pi z)\\
u^{3ds8} &= z\tanh((-\sin(x)+y^2))\\
u^{3dns1} &= |x^2+y^2+z^2|^{0.8}\\
u^{3dns2} &= (xe^{1-|x|}-x)(ye^{1-|y|}-y)(ze^{1-|z|}-z).
\end{aligned}$$

The maximum errors, mean squared errors of approximate spline solutions against the exact solution are computed based on $501 \times 501 \times 501$ equally-spaced points over

Domain	Number of vertices	Number of triangles	Average time for AWL method	Average time for LL method (part 2)
Gear	274	426	4.7290e+01	9.3832e-01
Flower with a hole	297	494	1.7610e+01	1.0522e+00
Montreal	549	870	2.6441e+01	1.5352e+00
Circle with 3 holes	525	895	3.0227e+01	1.6433e+00

TABLE 6

The number of vertices, triangles and the averaged time for solving the 2D Poisson equation for each domain in Figure 1.

	L shaped domain		Human head		Torus		Letter B	
Solution	RMSE	error	RMSE	error	RMSE	error	RMSE	error
u^{3ds1}	3.15e-11	9.69e-11	5.83e-12	6.45e-11	1.79e-10	2.04e-09	6.86e-12	4.11e-11
u^{3ds2}	8.21e-10	2.15e-09	3.45e-10	2.95e-09	1.14e-08	8.50e-08	4.50e-11	6.24e-10
u^{3ds3}	7.33e-10	2.37e-09	7.26e-10	8.21e-09	5.34e-09	3.31e-08	3.96e-09	3.48e-07
u^{3ds4}	3.89e-10	1.06e-09	2.68e-10	2.76e-09	3.57e-09	2.29e-08	7.89e-11	1.36e-09
u^{3ds5}	1.02e-09	2.88e-09	9.75e-10	5.78e-09	1.33e-08	8.95e-08	3.64e-09	4.16e-07
u^{3ds6}	3.86e-09	1.10e-08	2.35e-09	2.47e-08	3.39e-08	1.90e-07	3.65e-10	2.63e-09
u^{3ds7}	1.76e-09	1.49e-08	4.19e-08	5.21e-07	1.01e-07	2.34e-06	4.86e-08	4.39e-07
u^{3ds8}	5.89e-11	1.94e-10	2.69e-11	1.66e-10	6.42e-10	4.32e-09	8.16e-11	1.52e-09
u^{3dns1}	1.15e-06	9.60e-05	3.82e-06	6.23e-04	5.07e-09	3.22e-08	7.98e-07	1.34e-04
u^{3dns2}	5.49e-06	9.37e-05	2.30e-04	4.84e-03	1.09e-04	1.58e-03	5.51e-06	2.06e-04

TABLE 7

The RMSE and the maximum errors of spline solutions for the 3D Poisson equation over the four domains in Figure 2 when $r = 1$ and $D = 9$.

the different domains shown Figure 2.

We choose collocation points to create $2m \times m$ matrix K, where m is the number of Bernstein basis functions, i.e. the dimension of spline space $S_D^{-1}(\triangle)$ and used the iterative method to find the numerical solutions. We tested 10 functions over the domains in Figure 2 and present the maximum errors, root mean square error(RMSE) are presented in Table 7. We also compare the AWL method and LL method for the numerical solution of the 3D Poisson equation. See numerical results in Table 8 and 9.

7. Numerical Results for General Second Order Elliptic PDE. We shall present computational results for 2D general second order PDEs and 3D general second order PDEs separately in the following two subsections. In each section, we first present the computational results from the spline based collocation method to demonstrate the accuracy the method can achieve. Then we present a comparison of our collocation method with the numerical method based on [12]. For convenience, we shall call our spline based collocation method the LL method and the numerical method in [12] the LW method.

7.1. Numerical examples for 2D general second order equations. We have used the same triangulations over various bounded domains as shown in Figure 1 and tested the same solutions which we used for the Poisson equation for the general second order equation to see the accuracy that the LL method can have. The maximum errors and the root mean squared error(RMSE) of approximate spline solutions against the exact solution are given in Tables in this section. The maximum errors are computed based on 501×501 equally-spaced points fell inside the different domains in Figure 1. We chose additional collocation points to create $2m \times m$ matrix $\mathcal{K}$, where m is the number of Bernstein basis functions (the dimension of spline space $S_D^{-1}(\triangle)$ and used the similar iterative method in [1] to find the numerical solutions.

	L shaped domain				Human head			
	AWL		LL		AWL		LL	
Solution	RMSE	error	RMSE	error	RMSE	error	RMSE	error
u^{3ds1}	8.64e-12	2.07e-10	3.15e-11	9.69e-11	2.83e-09	7.56e-07	5.83e-12	6.45e-11
u^{3ds2}	2.54e-10	4.92e-09	8.21e-10	2.15e-09	1.61e-08	2.72e-06	3.45e-10	2.95e-09
u^{3ds3}	1.37e-10	3.51e-09	7.33e-10	2.37e-09	6.44e-08	1.21e-05	7.26e-10	8.21e-09
u^{3ds4}	1.16e-10	2.09e-09	3.89e-10	1.06e-09	1.83e-08	2.72e-06	2.68e-10	2.76e-09
u^{3ds5}	2.70e-10	3.89e-09	1.02e-09	2.88e-09	6.09e-08	8.43e-06	9.75e-10	5.78e-09
u^{3ds6}	8.56e-10	1.04e-08	3.86e-09	1.10e-08	1.31e-07	1.35e-05	2.35e-09	2.47e-08
u^{3ds7}	2.61e-10	2.90e-09	1.76e-09	1.49e-08	1.88e-08	2.72e-06	4.19e-08	5.21e-07
u^{3ds8}	1.79e-11	4.96e-10	5.89e-11	1.94e-10	8.16e-09	3.41e-07	2.69e-11	1.66e-10
u^{3dns1}	5.86e-05	3.61e-03	1.15e-06	9.60e-05	3.63e-08	2.67e-06	3.82e-06	6.23e-04
u^{3dns2}	1.67e-03	3.87e-03	5.49e-06	9.37e-05	3.42e-04	2.49e-03	2.30e-04	4.84e-03

TABLE 8

The maximum errors of spline solutions for the 3D Poisson equation over the four domains in Figure 2 when $r = 1$ and $D = 9$ for the AWL method and LL method.

	Torus				Letter B			
	AWL		LL		AWL		LL	
Solution	RMSE	error	RMSE	error	RMSE	error	RMSE	error
u^{3ds1}	3.55e-09	5.74e-07	1.79e-10	2.04e-09	4.35e-11	1.43e-09	6.86e-12	4.11e-11
u^{3ds2}	2.92e-08	1.98e-06	1.14e-08	8.50e-08	3.71e-10	5.42e-09	4.50e-11	6.24e-10
u^{3ds3}	1.07e-07	8.90e-06	5.34e-09	3.31e-08	6.08e-10	4.45e-08	3.96e-09	3.48e-07
u^{3ds4}	1.88e-08	1.46e-06	3.57e-09	2.29e-08	9.06e-11	1.11e-09	7.89e-11	1.36e-09
u^{3ds5}	8.25e-08	5.50e-06	1.33e-08	8.95e-08	5.72e-10	5.57e-08	3.64e-09	4.16e-07
u^{3ds6}	2.50e-07	1.80e-05	3.39e-08	1.90e-07	7.19e-10	1.36e-08	3.65e-10	2.63e-09
u^{3ds7}	8.07e-08	5.83e-06	1.01e-07	2.34e-06	4.95e-09	1.15e-07	4.86e-08	4.39e-07
u^{3ds8}	8.16e-09	7.24e-07	6.42e-10	4.32e-09	6.73e-11	1.77e-09	8.16e-11	1.52e-09
u^{3dns1}	3.92e-08	2.67e-06	5.07e-09	3.22e-08	3.24e-04	9.12e-03	7.98e-07	1.34e-04
u^{3dns2}	6.30e-04	2.29e-03	1.09e-04	1.58e-03	1.18e-03	3.97e-03	5.51e-06	2.06e-04

TABLE 9

The maximum errors and root mean square error(RMSE) of spline solutions for the 3D Poisson equation over the four domains in Figure 2 when $r = 1$ and $D = 9$ for the AWL method and LL method.

7.1.1. 2D general second order equations with smooth coefficients. We first tested a 2nd order elliptic equation with smooth coefficients with $a_{11} = x^2 + y^2, a_{12} = \cos(xy), a_{21} = e^{xy}, a_{22} = x^3 + y^2 - sin(x^2 + y^2), b_1 = 3\cos(x)y^2, b_2 = e^{-x^2-y^2}, c = 0$. Using these smooth coefficients, we have tested 2 non-smooth solutions u^{ns1}, u^{ns2}, and 8 smooth solutions $u^{s1} - u^{s8}$ for our four domains used in the previous section. And the errors of the solutions for the four domains in Figure 1 is presented in Table 11. The numerical results show that the LL method works very well. In Table 12, we compare with the LW method and see that the LL method produces more accurate results.

Finally, Table 13 shows the averaged computational time for the LL method is shorter than the LW method. Together with the computational results in Table 12, we conclude that the LL method is more effective and efficient than the LW method.

7.1.2. 2D general second order equations with non-smooth coefficients.

EXAMPLE 1. *In [18], the researchers experimented their numerical methods for the second order PDE as follows:*

$$\sum_{i,j=1}^{2} (1 + \delta_{ij}) \frac{x_i}{|x_i|} \frac{x_j}{|x_j|} u_{x_i x_j} = f \quad in\ \Omega, \quad u = 0\ on\ \partial\Omega,$$

Domain	Number of vertices	Number of tetrahedrons	Average time for AWL method	Average time for LL method
L-shaped domain	325	1152	6.9400e+02	9.6791e+01
Human head	913	1588	3.7610e+03	1.0729e+02
Torus	773	2911	4.5198e+03	4.5197e+02
Letter B	299	816	2.6495e+02	3.7484e+01

TABLE 10

The number of vertices, tetrahedrons and the averaged time for solving the 3D Poisson equations for each domain in Figure 2.

	Gear		Flower with a hole		Montreal		Circle with 3 holes	
Solns	RMSE	error	RMSE	error	RMSE	error	RMSE	error
u^{s1}	3.48e-10	1.08e-09	2.43e-10	1.52e-09	8.13e-11	3.87e-10	8.84e-11	3.80e-10
u^{s2}	1.79e-08	6.07e-08	1.65e-06	9.04e-06	1.81e-10	8.90e-10	4.61e-11	1.65e-10
u^{s3}	1.21e-10	4.80e-10	3.61e-11	1.95e-10	9.91e-11	5.30e-10	2.67e-11	1.12e-10
u^{s4}	1.45e-08	5.69e-08	1.02e-06	4.87e-06	7.80e-11	3.59e-10	5.40e-11	1.97e-10
u^{s5}	1.87e-07	7.00e-07	1.94e-06	1.38e-05	1.94e-11	8.54e-11	9.65e-11	3.67e-10
u^{s6}	3.00e-08	1.75e-07	4.44e-06	3.27e-05	2.91e-12	9.90e-12	2.97e-11	1.37e-10
u^{s7}	2.54e-11	7.55e-11	6.50e-12	2.66e-11	1.42e-11	6.08e-11	4.15e-12	1.55e-11
u^{s8}	1.52e+00	5.85e+00	9.77e+00	5.41e+01	9.61e-08	9.79e-07	2.66e-03	1.19e-02
u^{ns1}	2.43e-05	1.83e-03	1.01e-10	4.22e-10	1.55e-06	9.63e-05	2.05e-04	9.33e-03
u^{ns2}	1.22e-04	8.20e-04	1.97e-04	1.33e-03	5.30e-06	4.22e-05	3.87e-05	2.92e-04

TABLE 11

The maximum errors and RMSE of spline solutions for general second order elliptic equations with smooth coefficients over the each domain in Figure 1 when $r = 2$ and $D = 8$.

where $\Omega = (-1,1)^2$ and the solution u is $u(x,y) = (xe^{1-|x|} - x)(ye^{1-|y|} - y)$ which is one of our testing functions. It is easy to see those coefficients satisfy the Cordes condition

$$\frac{\sum_{i,j=1}^{d}(a_{i,j})^2}{(\sum_{i=1}^{2} a_{ii})^2} = \frac{2^2+1+1+2^2}{(2+2)^2} = \frac{10}{16} \leq \frac{1}{2-1+\epsilon}$$

when $\epsilon = \frac{3}{5}$. This equation was also numerically experimented in [12] and [19].

Let us test our method on this 2nd order elliptic equation with non-smooth coefficients for the 2 non-smooth solutions u^{ns1}, u^{ns2}, and 8 smooth solutions $u^{s1} - u^{s8}$ over the four domains used in the previous section. We use bivariate splines of degree $D = 8$ and smoothness $r = 2$. And the maximum errors and RMSE of the solutions for the four domains in Figure 1 are presented in Table 14. Table 15 shows that LL method produces solutions with better accuracy than LW method over these 4 domains.

EXAMPLE 2. *The second example in the paper [18] is another second order PDE:*

$$\sum_{i,j=1}^{2}(\delta_{ij} + \frac{x_i x_j}{|x|^2})u_{x_i x_j} = f \quad in\ \Omega, \quad u = 0\ on\ \partial\Omega,$$

where $\Omega = (0,1)^2$ and the solution u is $u(x,y) = |x^2+y^2|^{\frac{\alpha}{2}}$ which is on the list of our testing functions. Then those coefficients satisfy the Cordes condition when $\epsilon = \frac{4}{5}$.

Similar to Example 1, we also tested solving the PDE by using the 10 testing functions used before with $D = 8$ and $r = 2$. See Table 16 for the maximum and RMSE errors. Table 17 shows that the LL method produces numerical solutions with a better accuracy than that of the LW method over these 4 domains.

7.1.3. Numerical Results for 3D General Second Order Elliptic Equations. In this subsection, we extend the PDE in Example 1–Example 2 to the 3D

	Gear		Flower with a hole		Montreal		Circle with 3 holes	
Solns	LW	LL	LW	LL	LW	LL	LW	LL
u^{s1}	1.28e-06	1.08e-09	8.93e-08	1.52e-09	2.21e-07	3.87e-10	1.36e-08	3.80e-10
u^{s2}	3.88e-06	6.07e-08	8.36e-07	9.04e-06	4.95e-07	8.90e-10	1.60e-07	1.65e-10
u^{s3}	5.98e-07	4.80e-10	2.10e-08	1.95e-10	2.48e-07	5.30e-10	1.32e-08	1.12e-10
u^{s4}	7.97e-06	5.69e-08	1.09e-06	4.87e-06	2.45e-07	3.59e-10	1.77e-07	1.97e-10
u^{s5}	9.51e-05	7.00e-07	3.50e-06	1.38e-05	6.97e-08	8.54e-11	3.80e-07	3.67e-10
u^{s6}	2.96e-05	1.75e-07	1.43e-07	3.27e-05	8.09e-09	9.90e-12	1.77e-08	1.37e-10
u^{s7}	1.90e-08	7.55e-11	4.16e-09	2.66e-11	3.51e-08	6.08e-11	1.86e-09	1.55e-11
u^{s8}	1.17e+00	5.85e+00	1.75e+00	5.41e+01	6.18e-07	9.79e-07	5.80e-03	1.19e-02
u^{ns1}	9.85e-02	1.83e-03	9.24e-04	4.22e-10	6.91e-05	9.63e-05	8.07e-04	9.33e-03
u^{ns2}	4.95e-02	8.20e-04	1.02e-02	1.33e-03	1.85e-04	4.22e-05	1.80e-03	2.92e-04

TABLE 12

The maximum errors of spline solutions for general elliptic equations with smooth coefficients over the four domains studied before when $r = 2$ and $D = 8$ for the LW method and the LL method.

Domain	Number of vertices	Number of triangles	Average time for LW method	Average time for Part 2 of LL method
Gear	274	426	5.6646e+02	1.0355e+01
Flower with a hole	297	494	8.3236e+02	1.1792e+01
Montreal	549	870	1.9026e+03	2.5606e+01
Circle with 3 holes	525	895	4.4387e+03	2.6831e+01

TABLE 13

The number of vertices, triangles and the averaged time in seconds for solving 2D general second order equations over the four domains in Figure 1 by the LW and LL methods.

	Gear		Flower with a hole		Montreal		Circle with 3 holes	
Solution	RMSE	error	RMSE	error	RMSE	error	RMSE	error
u^{s1}	3.28e-10	7.65e-10	1.40e-11	4.90e-11	4.48e-10	1.50e-09	2.00e-11	7.49e-11
u^{s2}	1.29e-09	1.24e-08	9.50e-08	9.48e-07	9.31e-10	2.76e-09	2.78e-11	9.55e-11
u^{s3}	5.39e-11	2.76e-10	9.62e-12	4.66e-11	5.99e-10	2.11e-09	9.71e-12	3.21e-11
u^{s4}	1.37e-09	9.85e-09	1.17e-07	1.01e-06	1.21e-09	4.32e-09	4.66e-11	1.45e-10
u^{s5}	2.88e-08	9.74e-08	9.10e-08	3.18e-07	1.53e-10	5.38e-10	2.04e-11	6.88e-11
u^{s6}	5.71e-10	7.98e-09	8.40e-08	6.89e-07	5.32e-11	1.94e-10	8.36e-12	3.05e-11
u^{s7}	2.56e-11	1.08e-10	6.61e-13	2.67e-12	2.18e-11	1.88e-10	1.88e-12	6.52e-12
u^{s8}	6.49e-02	4.18e-01	4.23e-01	1.75e+00	7.14e-08	5.90e-07	1.43e-04	2.22e-03
u^{ns1}	1.74e-03	9.09e-03	3.61e-11	2.63e-10	1.06e-03	4.68e-03	2.33e-05	2.58e-04
u^{ns2}	5.50e-04	1.73e-03	2.87e-04	1.07e-03	7.09e-05	2.90e-04	8.11e-05	2.94e-04

TABLE 14

The maximum errors of spline solutions for general elliptic equations with non-smooth coefficients in Example 1 over the four domains in Figure 2 when $r = 2$ and $D = 8$.

	Gear		Flower with a hole		Montreal		Circle with 3 holes	
Method	LW	LL	LW	LL	LW	LL	LW	LL
u^{s1}	5.69e-05	7.65e-10	1.18e-04	4.90e-11	3.93e-08	1.50e-09	9.11e-06	7.49e-11
u^{s2}	8.94e-04	1.24e-08	1.99e-03	9.48e-07	1.61e-06	2.76e-09	1.39e-04	9.55e-11
u^{s3}	1.25e-04	2.76e-10	4.20e-05	4.66e-11	2.89e-07	2.11e-09	1.77e-05	3.21e-11
u^{s4}	1.72e-03	9.85e-09	1.97e-03	1.01e-06	3.92e-07	4.32e-09	2.19e-04	1.45e-10
u^{s5}	9.71e-03	9.74e-08	4.53e-03	3.18e-07	1.14e-02	5.38e-10	2.83e-02	6.88e-11
u^{s6}	1.12e-04	7.98e-09	5.08e-05	6.89e-07	2.51e-08	1.94e-10	1.48e-05	3.05e-11
u^{s7}	1.16e-05	1.08e-10	4.77e-06	2.67e-12	1.90e-05	1.88e-10	5.02e-05	6.52e-12
u^{s8}	7.90e-01	4.18e-01	1.07e+00	1.75e+00	2.22e-02	5.90e-07	6.34e-02	2.22e-03
u^{ns1}	6.97e-03	9.09e-03	3.92e-05	2.63e-10	1.19e-03	4.68e-03	3.72e-04	2.58e-04
u^{ns2}	8.17e-03	1.73e-03	1.78e-03	1.07e-03	6.78e-04	2.90e-04	1.61e-03	2.94e-04

TABLE 15

The maximum errors of spline solutions for general elliptic equations with non-smooth coefficients in Example 1 over the four domains when $r = 2$ and $D = 8$ for the LW method and the LL method.

This manuscript is for review purposes only.

	Gear		Flower with a hole		Montreal		Circle with 3 holes	
Solution	RMSE	error	RMSE	error	RMSE	error	RMSE	error
u^{s1}	1.74e-10	4.02e-10	8.49e-12	3.64e-11	1.24e-10	4.43e-10	1.19e-11	4.18e-11
u^{s2}	1.39e-09	1.07e-08	1.03e-07	9.29e-07	4.05e-10	1.25e-09	5.49e-12	1.89e-11
u^{s3}	1.29e-10	5.09e-10	9.32e-12	3.66e-11	3.03e-10	9.81e-10	3.04e-12	1.01e-11
u^{s4}	1.09e-09	9.22e-09	1.11e-07	9.37e-07	1.21e-10	4.47e-10	6.32e-12	2.44e-11
u^{s5}	1.75e-08	6.64e-08	1.06e-07	3.30e-07	1.02e-10	3.34e-10	1.03e-11	3.25e-11
u^{s6}	5.55e-10	9.07e-09	8.05e-08	4.91e-07	1.12e-11	5.97e-11	2.83e-12	9.33e-12
u^{s7}	5.16e-12	2.15e-11	7.14e-13	2.41e-12	2.46e-11	8.34e-11	8.19e-13	2.88e-12
u^{s8}	6.15e-02	3.65e-01	4.60e-01	2.05e+00	2.07e-08	3.67e-07	1.69e-04	3.00e-03
u^{ns1}	1.75e-03	9.35e-03	3.12e-11	1.89e-10	1.12e-04	7.52e-04	2.34e-05	3.47e-04
u^{ns2}	1.23e-04	5.80e-04	8.48e-05	5.70e-04	3.53e-06	1.60e-05	1.05e-05	1.15e-04

TABLE 16

The maximum errors and RMSE of spline solutions for general elliptic equations with non-smooth coefficients in Example 2 over the four domains when $r = 2$ and $D = 8$.

	Gear		Flower with a hole		Montreal		Circle with 3 holes	
Method	LW	LL	LW	LL	LW	LL	LW	LL
u^{s1}	2.11e-06	4.02e-10	1.19e-06	3.64e-11	4.55e-10	4.43e-10	3.61e-06	4.18e-11
u^{s2}	2.36e-05	1.07e-08	7.82e-06	9.29e-07	1.81e-08	1.25e-09	1.33e-05	1.89e-11
u^{s3}	4.98e-06	5.09e-10	2.60e-07	3.66e-11	3.83e-09	9.81e-10	1.79e-06	1.01e-11
u^{s4}	6.50e-06	9.22e-09	1.20e-05	9.37e-07	6.68e-10	4.47e-10	8.93e-06	2.44e-11
u^{s5}	4.32e-02	6.64e-08	1.37e-05	3.30e-07	1.35e-03	3.34e-10	5.46e-04	3.25e-11
u^{s6}	5.63e-03	9.07e-09	6.38e-07	4.91e-07	1.00e-04	5.97e-11	2.62e-05	9.33e-12
u^{s7}	6.57e-05	2.15e-11	7.89e-08	2.41e-12	1.90e-06	8.34e-11	7.68e-07	2.88e-12
u^{s8}	4.54e-01	3.65e-01	8.85e-01	2.05e+00	4.51e-03	3.67e-07	2.78e-03	3.00e-03
u^{ns1}	7.18e-03	9.35e-03	4.15e-07	1.89e-10	1.03e-03	7.52e-04	3.22e-04	3.47e-04
u^{ns2}	6.99e-03	5.80e-04	9.81e-04	5.70e-04	1.40e-04	1.60e-05	3.86e-04	1.15e-04

TABLE 17

The maximum errors of spline solutions for general elliptic equations with non-smooth coefficients in Example 2 over the four domains when $r = 2$ and $D = 8$ for the LW method and the LL method.

setting and use our collocation method based on trivariate splines to find spline approximation.

EXAMPLE 3. *We tested a 2nd order elliptic equation (1.2) with smooth PDE coefficients $a_{11} = x^2 + y^2, a^{22} = \cos(xy - z), a^{33} = \exp(\frac{1}{x^2+y^2+z^2+1}), a^{12} + a^{21} = x^2 - y^2 - z, a^{23} + a^{32} = \cos(xy - z)\sin(x - y), a^{13} + a^{31} = \frac{1}{y^2+z^2+1}, b_1 = 0, b_2 = -1, b_3 = \tan^{-1}(x^3 - y^2 + \cos(z)), c = x + y + z$, where $a^{12} = a^{21}, a^{32} = a^{23}$ and $a^{13} = a^{31}$. The testing functions are the 2 not very smooth solutions u^{ns1}, u^{ns2}, and 8 smooth solutions $u^{s1} - u^{s8}$ over the four domains used in the previous section. And the maximum and RMSE errors of the solutions for the four domains in Figure 2 are reported in Table 18.*

EXAMPLE 4. *We next test a 3D general second order equations with nonsmooth PDE coefficients:*

$$\sum_{i,j=1}^{3} (1 + \delta^{ij}) \frac{x_i}{|x_i|} \frac{x_j}{|x_j|} u_{x_i x_j} = f \quad in\ \Omega, \quad u = 0\ on\ \partial\Omega$$

which is an extension of one of the examples studied in [18]. These PDE coefficients satisfies the Cordes condition

$$\frac{\sum_{i,j=1}^{3} (a^{i,j})^2}{(\sum_{i=1}^{3} a^{ii})^2} = \frac{2^2 + 1 + 1 + 2^2 + 1 + 1 + 2^2 + 1 + 1}{(2 + 2 + 2)^2} = \frac{18}{64} \leq \frac{1}{3 - 1 + \epsilon}$$

	L shaped domain		Human head		Torus		Letter B	
Solution	RMSE	error	RMSE	error	RMSE	error	RMSE	error
u^{s1}	2.08e-11	1.32e-10	5.04e-12	3.70e-11	1.48e-11	1.53e-10	3.07e-12	3.19e-11
u^{s2}	5.07e-10	3.02e-09	6.98e-10	4.07e-09	7.53e-10	4.77e-09	3.80e-11	3.00e-10
u^{s3}	2.88e-10	1.85e-09	1.73e-09	1.52e-08	1.72e-09	2.43e-08	3.41e-08	4.85e-07
u^{s4}	2.23e-10	1.24e-09	7.73e-10	6.34e-09	3.83e-10	2.17e-09	2.63e-10	4.04e-09
u^{s5}	6.73e-10	3.93e-09	1.20e-09	8.54e-09	1.83e-09	3.66e-08	1.58e-08	3.89e-07
u^{s6}	1.55e-09	9.42e-09	5.62e-09	4.81e-08	4.55e-09	2.25e-08	1.73e-10	1.47e-09
u^{s7}	4.00e-09	2.13e-07	1.12e-07	9.35e-07	9.21e-08	3.70e-06	8.26e-08	1.02e-06
u^{s8}	1.81e-11	1.04e-10	3.76e-11	2.45e-10	5.52e-11	3.99e-10	6.43e-11	1.46e-09
u^{ns1}	5.27e-06	1.64e-04	1.23e-05	4.15e-04	8.61e-10	6.61e-09	1.03e-05	2.26e-04
u^{ns2}	6.99e-05	1.05e-03	1.86e-04	2.62e-03	1.25e-04	1.75e-03	3.55e-05	4.45e-04

TABLE 18

The maximum errors and the root mean square error(RMSE) of spline solutions of the general elliptic 2nd order equation in Example 3 with smooth coefficients over the four domains in Figure 2 when $r = 1$ and $D = 9$.

	L shaped domain		Human head		Torus		Letter B	
Solution	RMSE	error	RMSE	error	RMSE	error	RMSE	error
u^{s1}	3.05e-06	1.14e-04	1.75e-12	1.97e-11	1.82e-05	2.02e-04	1.94e-05	6.21e-04
u^{s2}	2.92e-05	6.98e-04	1.86e-10	1.31e-09	4.55e-04	3.77e-03	1.26e-04	3.29e-03
u^{s3}	2.08e-04	6.26e-03	3.67e-10	4.06e-09	3.54e-03	2.74e-02	7.09e-04	2.30e-02
u^{s4}	1.17e-05	3.28e-04	1.23e-10	8.40e-10	1.20e-04	9.87e-04	1.88e-05	4.84e-04
u^{s5}	1.52e-04	4.03e-03	6.92e-10	4.24e-09	2.81e-03	2.73e-02	6.15e-04	2.10e-02
u^{s6}	1.45e-04	3.72e-03	1.21e-09	1.08e-08	2.32e-03	1.84e-02	2.58e-04	5.63e-03
u^{s7}	1.96e-09	1.67e-08	4.42e-08	5.16e-07	1.04e-07	2.53e-06	4.18e-08	4.90e-07
u^{s8}	6.75e-06	2.59e-04	5.38e-12	3.93e-11	4.79e-05	4.96e-04	2.02e-05	5.46e-04
u^{ns1}	2.46e-05	5.11e-04	1.73e-05	1.12e-03	4.55e-04	3.72e-03	5.06e-05	7.59e-04
u^{ns2}	6.88e-13	3.63e-12	9.30e-05	1.78e-03	1.07e-04	1.69e-03	1.08e-13	8.11e-13

TABLE 19

The maximum errors and the RMSE of spline solutions for the general elliptic 2nd order equations in Example 4 with non-smooth coefficients over the four domains in Figure 2 when $r = 1$ and $D = 9$.

when $\epsilon \leq 1$. We tested our splined based collocation method using the 2 not very smooth solutions u^{ns1}, u^{ns2}, and 8 smooth solutions from u^{s1} to u^{s8} given in the previous section. over the four domains used before with $D = 9$ and $r = 1$. And the errors of the solutions for the four domains in Figure 2 are presented in Table 19.

EXAMPLE 5. *We consider the second example in [18] and extend it to the 3D setting:*

$$\sum_{i,j=1}^{3} (\delta_{ij} + \frac{x_i x_j}{|\mathbf{x}|^2}) u_{x_i x_j} = f \quad in\ \Omega, \quad u = 0\ on\ \partial\Omega$$

Note that these PDE coefficients satisfy the Cordes condition when $\epsilon = \frac{4}{5}$. We use our collocation method and tested 2 not-very-smooth solutions u^{ns1}, u^{ns2}, and 8 smooth solutions $u^{s1} - -u^{s8}$ over the 4 domains used before with $D = 9$ and $r = 1$. The maximum and RMSE errors are presented in Table 20.

From Tables 18–20, we can see that the collocation method works very well in the 3D setting.

REFERENCES

[1] G. Awanou, M. -J. Lai, and P. Wenston, The multivariate spline method for scattered data fitting and numerical solution of partial differential equations. In Wavelets and splines: Athens 2005, pages 24–74. Nashboro Press, Brentwood, TN, 2006.

	L shaped domain		Human head		Torus		Letter B	
Solution	RMSE	error	RMSE	error	RMSE	error	RMSE	error
u^{s1}	5.46e-12	4.60e-11	3.21e-12	3.94e-11	1.01e-10	1.11e-09	3.95e-12	1.33e-10
u^{s2}	1.11e-10	7.06e-10	2.95e-10	2.75e-09	6.74e-09	3.94e-08	3.59e-11	1.09e-09
u^{s3}	1.04e-10	1.13e-09	5.74e-10	5.80e-09	2.68e-09	3.71e-08	8.93e-09	8.33e-07
u^{s4}	4.52e-11	3.99e-10	2.13e-10	1.31e-09	3.79e-09	2.25e-08	5.10e-11	9.62e-10
u^{s5}	1.12e-10	1.11e-09	8.06e-10	7.05e-09	7.62e-09	5.03e-08	8.68e-09	9.36e-07
u^{s6}	6.58e-10	2.92e-09	2.25e-09	1.73e-08	2.68e-08	1.33e-07	1.79e-10	3.58e-09
u^{s7}	1.89e-09	3.72e-08	4.46e-08	5.87e-07	1.53e-07	4.18e-06	5.50e-08	1.22e-06
u^{s8}	8.87e-12	5.78e-11	1.90e-11	1.16e-10	3.08e-10	2.68e-09	6.02e-11	1.03e-09
u^{ns1}	4.88e-06	2.92e-04	1.62e-05	1.07e-03	3.47e-09	2.31e-08	3.76e-06	2.04e-04
u^{ns2}	4.31e-05	1.88e-04	1.68e-04	3.79e-03	1.17e-04	1.58e-03	2.00e-05	4.21e-04

TABLE 20

The maximum errors and the RMSE of spline solutions for the general elliptic 2nd order equation with non-smooth coefficients in Example 5 over the four domains in Figure 2 when $r = 1$ and $D = 9$.

[2] H. Brezis, Functional analysis, Sobolev spaces and partial differential equations, Springer, 2011.

[3] P. Cummings and X. B. Feng, Shape regularity coefficient estimates for complex-valued acoustic and elastic Helmholtz equations, Math. Models Methods in Applied Sciences, 16(2006), 139–160.

[4] L. Evens, Partial Differential Equation. American Mathematical Society, Providence (1998)

[5] F. Gao and M. -J. Lai, A new H^2 regularity condition of the solution to Dirichlet problem of the Poisson equation and its applications, Acta Mathematica Sinica, vol. 36 (2020) pp. 21–39.

[6] P. Grisvard, Ellitpic Problems in Nonsmooth Domains, Pitman, 1985.

[7] X.-L. Hu, D.-F. Han, and M.-J Lai, Bivariate Splines of Various Degrees for Numerical Solution of Partial Differential Equations, SIAM J. Sci. Comput., 29(3), 1338–1354. (2007)

[8] M. -J. Lai, *On Construction of Bivariate and Trivariate Vertex Splines on Arbitrary Mixed Grid Partitions*, Dissertation, Texas A&M University, 1989.

[9] M. -J. Lai and Mersmann, C., Adaptive Triangulation Methods for Bivariate Spline Solutions of PDEs, Approximation Theory XV: San Antonio, 2016, edited by G. Fasshauer and L. L. Schumaker, Springer Verlag, (2017), pp. 155–175.

[10] M. -J. Lai and L. L. Schumaker, *Spline Functions over Triangulations*, Cambridge University Press, 2007.

[11] M. -J. Lai and L. L. Schumaker, Trivariate C^r polynomial macro-elements. Constr. Approx. 26 (2007), no. 1, 11–28.

[12] M. -J. Lai and Wang, C. M., A bivariate spline method for 2nd order elliptic equations in non-divergence form, Journal of Scientific Computing , (2018) pp. 803–829.

[13] M. -J. Lai and Y. Wang, Sparse Solutions of Underdetermined Linear Systems and Their Applications, SIAM Publication, Philadelphia (2021).

[14] J. Lee, A Multivariate Spline Method for Numerical Solution of Partial Differential Equations, Dissertation (under preparation), University of Georgia, 2022.

[15] L. Mu and X. Ye, A simple finite element method for non-divergence form elliptic equations, International Journal of Numerical Analysis and Modeling 14(2)(2017), pp. 306–311.

[16] L. L. Schumaker, Spline Functions: Computational Methods. SIAM Publication, Philadelphia (2015).

[17] L. L. Schumaker, Solving elliptic PDE's on domains with curved boundaries with an immersed penalized boundary method. J. Sci. Comput. 80 (2019), no. 3, 1369–1394.

[18] I. Smears, and E. Süli, Discontinuous Galerkin finite element approximation of nondivergence form elliptic equations with Cordes coefficients. SIAM J. Numer. Anal. 51(4), 2088–2106 (2013).

[19] C. Wang, J. Wang, A primal dual weak Galerkin finite element method for second order elliptic equations in non-divergence form, Math. Comp. 87 (2018), no. 310, 515–545.